Design, Build and Test of an Automated Fogponic Machine

Eduardo Camacho, Ethan Grocott, Parth Mittal, Saro Tchetchenian, Filippo Multari

Summary (FM)

Urbanisation and increasing reliance on international agricultural supply chains have introduced vulnerabilities to local food security. While consumer crop-growing systems already exist, they often lack precise environmental control. The project addresses this gap in the consumer market by designing, building, and functionally verifying an initial-stage, open source fogponics machine aimed at domestic users.

The resulting physical prototype is a compact farming unit, measuring 85cm tall with a 35x30cm base, primarily manufactured using 3D printing to enable rapid design iteration. At the top of this assembly sits a 1.7MHz ultrasonic atomizer responsible for mist generation, while an integrated Arduino R4 Wi-Fi microcontroller is used to process data from the required sensors. Prior to manufacturing, Computational Fluid Dynamics (CFD) simulations were also conducted to validate the design's fluid behaviour and functionality.

System testing successfully verified the hardware and automated control logic work, proving the machine reacts as intended to environmental changes and potential fault states. While extensive mechanical testing was conducted, time constraints prevented testing on plants. Consequently, integration of nutrients, LEDs growing lights, and plant chamber environmental control were excluded from the scope of the initial prototype.

In conclusion, the project successfully demonstrated the mechanical and electronical feasibility of an automated fogponics system, while highlighting critical adjustments for future iterations. Moving forward, the development should focus on transitioning the physical structure from 3D to scalable manufacturing processes, integration of nutrients and redesign of the atomization module.

Supervised by Dr M. Goudswaard

School of Electrical, Electronic, and Mechanical Engineering

University of Bristol

2026

Declaration

This project report is submitted towards an application for a degree at the University of Bristol. The report is based upon independent work by the candidates. All contributions from others have been acknowledged and the supervisor is identified on the front page. The views expressed within the report are those of the authors and not of the University of Bristol.

We hereby assert our right to be identified as the authors of this report. We give permission to the University of Bristol Library to add this report to its stock and to make it available for consultation in the library, and for inter-library lending for use in another library. It may be copied in full or in part for any bona fide library or research worker on the understanding that users are made aware of their obligations under copyright legislation.

We hereby declare that the above statements are true.

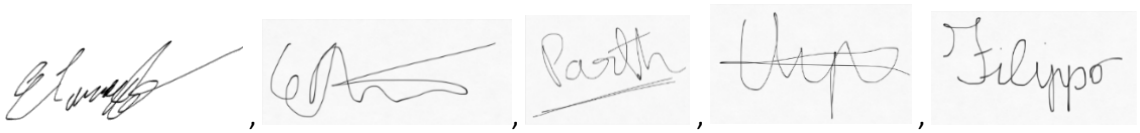

Work Allocation

	Eduardo Camacho (EC)	Ethan Grocott (EG)	Parth Mittal (PM)	Saro Tchetchenian (ST)	Filippo Multari (FM)
Summary					
Context and Motivation					
Literature Review					
Methodology					
Product Design Specification (PDS)					
Concept Generation and Selection					
System Decomposition					
Structural Design					
Atomiser Selection					
Sensors Selection					
Microcontroller and Programming					
Characterising Environmental Conditions of Growing Environment					
Detailed Design					
Test Plan					
Test Set-up					
Results and Evaluation					
Nutrients and pH					
Water Oxygenation					
Conclusion					

Key:

	Member has done the majority or the entire work on this section
	Member has contributed to this section
	Member has given feedback and reviewed this section

We confirm that the information on this page accurately describes our individual contributions to the project.

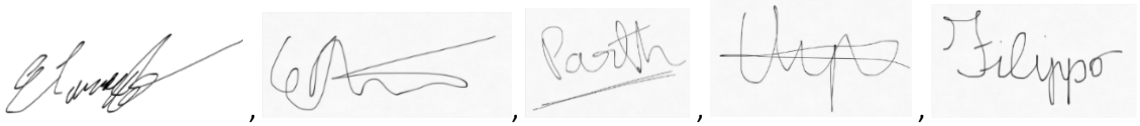

Contents

Table of Contents

1 Introduction

1.1 Context and Motivation (EG)

Urbanisation has spurred a transformation in the food production industry. As population densities increase, large-scale agricultural systems and extended supply and distribution chains can prove more economical than investing in local growers. In the UK, many crops are sourced through international supply chains to maintain year-round availability; for example, tomatoes are predominantly imported, with the Netherlands and Morocco alone accounting for 65% of supply. Whilst efficient at scale, this model increases dependence on complex logistics networks to ensure consistent supply.

The UK "hungry gap" describes a period from April to early June where locally grown crops are scarce [2]. During such periods, disruptions in supply chains can significantly affect both the availability and cost of produce. As a result, consumers have limited control over both the consistency and affordability of their food supply.

Consumer crop-growing systems have emerged to partially address this by enabling small-scale cultivation in an urban home. The core value proposition is to provide an economical and stable alternative to purchasing fresh produce, whilst appealing to environmentally conscious individuals by eliminating carbon emissions associated with food distribution. These systems can be effective in providing a plug-and-play experience with minimal user oversight. Although this simplicity is often achieved with limited control over the growing environment, with crops exposed directly to ambient room conditions. As a result, crop leaves are exposed to dust, odours and pets, and growth can be inconsistent and dependent on external factors such as temperature and airflow.

This highlights a gap in the consumer market: a controlled, self-contained system intended for use in a domestic setting that prioritises reliability, resource efficiency and yield rate. Therefore, the aim of this project is to develop an open-source, functional prototype to explore the overall feasibility of a solution within this niche, with consideration towards future commercialisation.

1.2 Literature Review (ST, FM)

To determine the optimal technology for a domestic and automated cultivating machine, six distinct farming methods were evaluated. The analysis has been summarised in *Table 1*.

Table 1 - Strengths and Weaknesses of the six different farming methods

Cultivating system	**Advantages**	**Disadvantages**
Deep-Water Culture (DWC) Hydroponics [1] Plant roots are constantly submerged in nutrient rich solution	- Constant supply of nutrients - Compact - Simplest hydroponic technique	- Poorest resilient due to high dependency on water aeration - Susceptible to software failure
Ebb and Flow Hydroponics [2] Plant roots are periodically flooded with nutrient rich solution	- Uses less water than indoor soil based (around 87% less) - Faster growth rate than traditional soil-based	- Higher possibility of salt build up than other hydroponic methods - Flood risk [3] - Susceptible to clogs in water pumps due to debris [4]
Nutrient Film Technique (NFT) Hydroponics [5] Shallow stream of nutrient rich solution recirculated past plant roots	- Faster growth rate than Ebb and Flow - More efficient water utilization than Ebb and Flow	- Susceptible to pathogen growth - Roots can cause water blockage of shallow nutrient film [6]
Indoor soil-based [7]	- Shield crops from urban air pollution;	- Adds substantial structural weight.

Plants are grown using soil	- Low-cost and requires minimal technical knowledge.	- Lower productivity per area used; - Increased risk of indoor pests and dirt.
Traditional aeroponics [8] Soil-less technique where plant roots are sprayed with high-pressure nozzles	- Precise environmental control and increased crop yields; - Good water efficiency.	- Complex and economically demanding structure; - High-pressure nozzles are prone to clogging; - High vulnerability to power interruptions;
Fogponics [9] Soil-less technique where ultrasonic atomizers are used to generate a fine mist	- Maximises root oxygenation for faster growth; - Good water efficiency (similar to traditional aeroponics).	- Requires precise and constant calibration of nutrient and pH; - Vulnerable to hardware failures and power interruptions.

This review served to establish a basic understanding of the agricultural techniques and their respective capabilities and limitations. However, at this stage, a final farming method has not yet been selected for development. The insights obtained from this literature review will directly be used for Concept Generation and Selection phase, where distinct concepts for each of this system will be analysed against the project's specific requirements.

2 Methodology (EC)

The development of a functional prototype followed a structured and iterative design methodology, as illustrated in *Figure 1*. The process began with problem definition and the establishment of requirements through a Product Design Specification (PDS). The Double Diamond design framework drove concept generation and evaluation, leading to the selection of a final design. The system was then developed through subsystem design and prototype construction. Testing and evaluation were conducted to assess system performance, with results informing iterative refinement of the design.

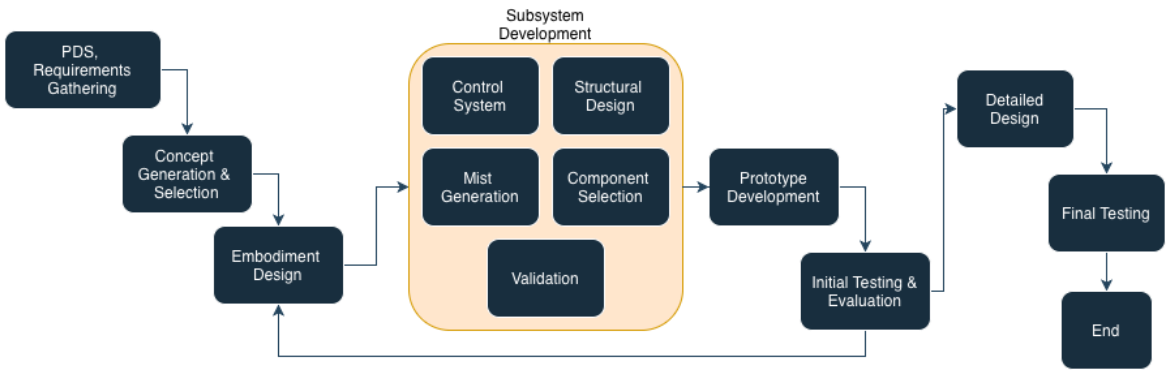

Figure 1 - Methodology Diagram

3 Product Design Specification (FM)

The Product Design Specification (PDS) outlined the essential requirements and constraints for the fogponics system. The design specifications were prioritised to focus on the needs of domestic users, categorising the requirements with Shall (requirement), Will (declaration of purpose), or Should (Goal) [10].

The PDS evolved continuously throughout the project. While the initial specifications defined broad operational goals, many more detailed requirements were introduced in response to the chosen farming technology. After the concepts was finalised, 41 total specifications were identified, and *Table 2* highlights the 10 most critical. The additional 31 requirements included in the completed PDS (shown in the eLogbook) have been omitted from this section because they address later stages of commercial product development, or are relevant to the automated nutrient delivery, which were excluded from the scope of the initial prototype.

Table 2 - PDS with the ten most important requirements

No.	Category	Requirement	Target/Limit	Priority	Test Method
1a	Structural Design, Sustainability, and Economics	1m height, 60cm width, and 40cm depth	Achieve within 5cm	Should	Measure the dimensions using a metre rule
1b		Blend with the decoration of the household	Wiring and plumbing must be enclosed within the main structure. Uniform surface finish	Must	Visual inspection of the fully assembled unit
2c	Plant growth and Root Environment	Keep humidity levels of root chamber high	More than 85% relative humidity in root chamber	Must	Testing with humidity sensor
2d		Absence of pests and algae	No visible pests or algae	Must	Test filtration system with dirty water
3a	Environmental control	System shall measure roots chamber's temperature accurately	±0.5°C	Must	Compare sensor reading with a thermometer
3b		The system shall measure Humidity of the roots chamber	±5%	Must	Use Sling Psychrometer to determine true relative humidity
4c	Mist generation	Dry-run protection for transducer	Auto-shutoff mechanism	Must	Drain tank during operation and time system's shutoff response
5a	Efficiency and Maintenance	Frequency of refill should be at least 5 days	8 litres water tank	Must	Test how long the system can last with a full tank
5i		The system notifies the user when main water reservoir requires refilling	Visual or auditory low alert at <20% capacity	Must	Slowly drain reservoir and verify that the alert triggers when water reaches threshold
6c	Microcontroller and Programming	The system shall control misting duration and interval with a resolution of 2 seconds	2 seconds	Must	Record the timings of several cycles

Ultimately, the PDS served as a foundation for the remainder of the development process. During the Concept Generation phase, the initial requirements have been used in the weighted Pugh Matrix, ensuring the selected farming technology aligned with the project's goals. The PDS also drove hardware selection and helped with developing the Test Plan.

4 Concept Generation and Selection

4.1 Concept Generation Methodology (EG)

Concept generation followed a Double Diamond framework. The first diamond focussed on determining which growing technology was best suited the project requirements. During the first divergent phase, one representative concept was generated for each candidate growing method. The following convergent phase employed a weighted Pugh matrix to evaluate these technologies and select the most suitable concept for further development.

The second diamond sought to refine the selected concept into a specific system configuration. Multiple configurations were generated and critically assessed against PDS requirements and for overall feasibility. The most suitable configuration was identified and brought forward into embodiment design.

4.2 Candidate Growing Technologies & Concepts (ST, EC, EG)

Six growing technologies were identified for comparison: enclosed soil culture, Deep Water Culture (DWC), Nutrient Film Technique (NFT), ebb-and-flow hydroponics, traditional high-pressure aeroponics and ultrasonic aeroponics (Fogponics). Each technology was represented by an initial, high-level concept. For brevity, only three representative concepts are illustrated in *Figures 2 to 4*: DWC, ebb-and-flow and Fogponics.

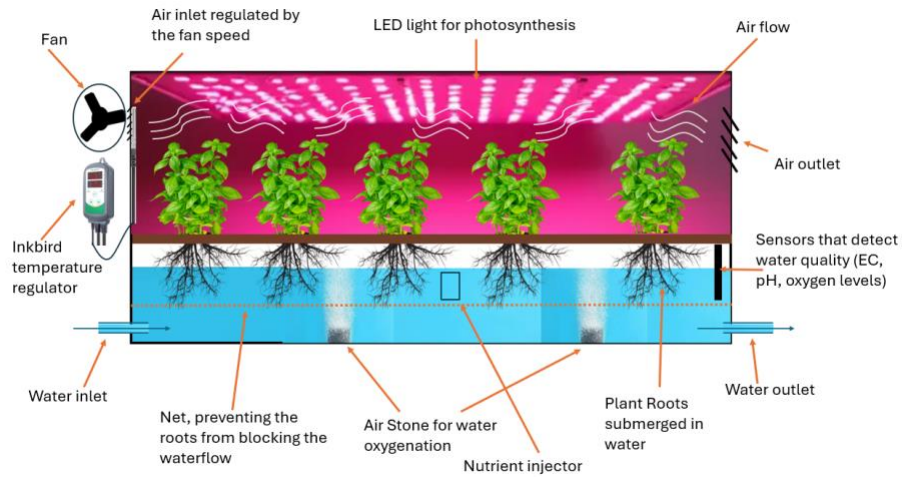

Figure 2 - DWC concept

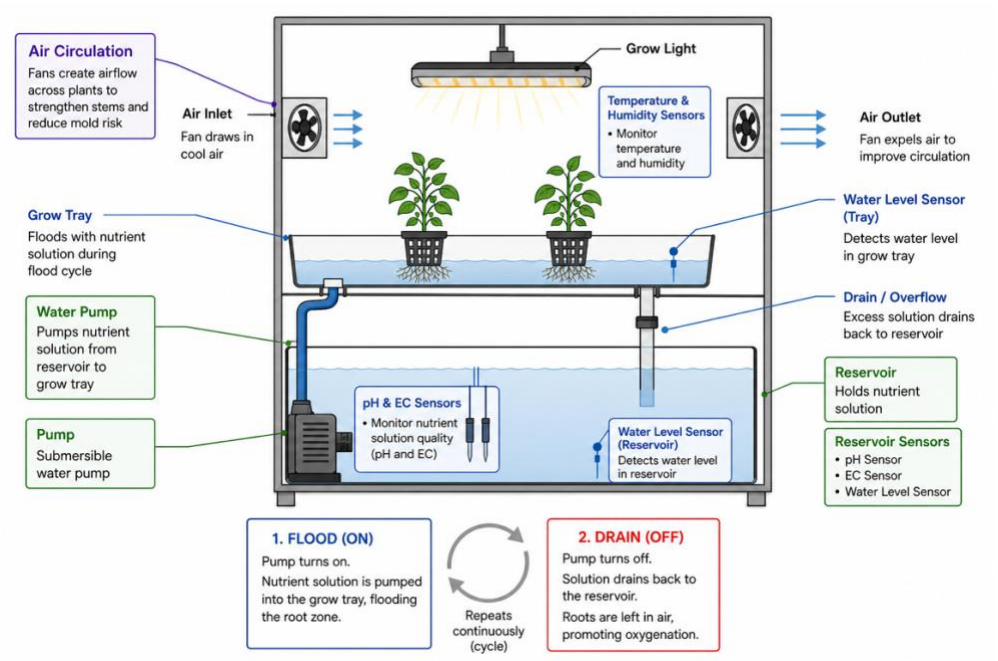

Figure 3 - Ebb and Flow Concept Diagram

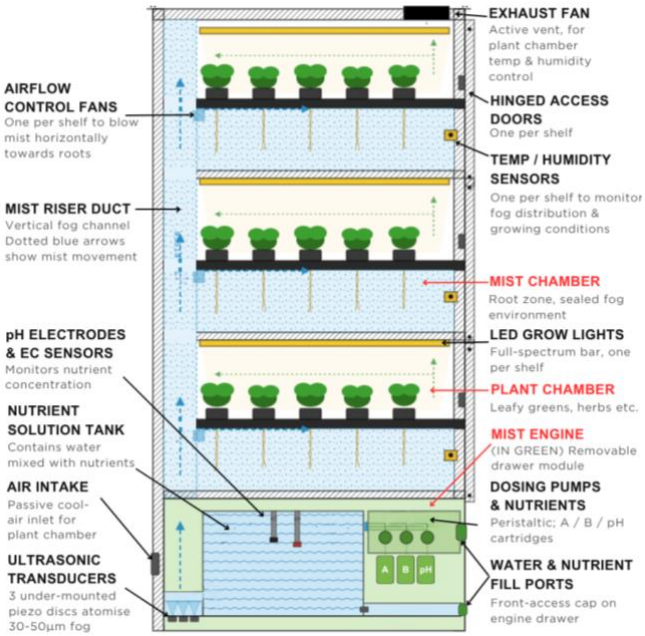

Figure 4 – Fogponic concept - side view

4.3 Concept Selection (PM, EG)

A total of 14 aspects were identified for the Pugh Matrix, shown in *Table 3*. These were derived from PDS requirements and weighted to reflect their importance to the final output. The comparison showed that Fogponics achieved the highest total score, with NFT emerging as the nearest competing concept. Soil-based cultivation scored lower due to poor level of automation, water efficiency and spatial efficiency. This result was intuitive; soil cultivation performs best in uncontrolled environments where its high biological buffer can be exploited. However, in small spaces, it is more feasible to deliver controlled nutrient dosage and ideal growing conditions, allowing for greater resource efficiency and improved nutrient absorption.

Consequently, hydroponic concepts, including DWC, NFT and ebb-and-flow, achieved higher resource efficiency and growth speed. They also demonstrated well balanced performance in a variety of other categories. The DWC concept was chosen as the datum since the technology is widely employed in commercial domestic growing solutions [11]. The ebb-and-flow concept showed promise in areas such as plant diversity and plant resilience due to the use of a growing medium. This allowed for a greater variety of plants to be grown without small inconsistencies in the growth process causing major issues. However, this can also introduce issues with disease and in a study [12] comparing NFT and ebb-and-flow, the ebb-and-flow technology produced lower yields over the same period of time as the NFT. Whilst the NFT concept required more auxiliary components than DWC, it did not require a large root zone. The roots could sweep the length of a water channel, achieving unparalleled spatial efficiency if scaled up. Whether this benefit could be sufficiently attained within the allotted dimensions was a point of contention. NFT also displayed the greatest growth speed amongst the considered hydroponic technologies.

Fogponic and Traditional Aeroponic systems share a common operating principle: both deliver nutrients by exposing plant roots to a fine mist of nutrient solution. This results in functionally equivalent growth speed and water efficiency, with both ranking highest among the evaluated concepts. The two technologies diverge in their method of mist generation. Traditional Aeroponics uses high-pressure pumps and spray nozzles, which are prone to clogging and demand frequent maintenance, undermining long-term reliability. Fogponics circumvents this drawback by generating mist through ultrasonic vibration using compact transducers. This offers reduced mechanical complexity, improved spatial efficiency and cheaper fabrication cost. Whilst mist-based root delivery maximises oxygen availability, it offers minimal resilience against power loss. Without periodic atomisation, the root zone desiccates rapidly, posing a significant risk to crop survival and overall system robustness.

Despite this vulnerability, the superior growth speed and water efficiency of Fogponics directly reinforce the core value proposition of the system. Coupled with its strong performance in other Pugh categories, the

risk of root zone desiccation was considered acceptable, given that operational interruptions were expected to be infrequent in an urban domestic setting. The Pugh Matrix result therefore supported Fogponics as the most suitable concept and growing technology.

Table 3 - Pugh Matrix

Pugh Matrix							
Critical Quality & Weighting	**DWC**	**NFT**	**Soil**	**Traditional Aeroponics**	**Fogponics**	**Ebb-and-Flow**	**Description**
Project Feasibility (1)	0	0	1	-1	-1	0	Ease of developing the system (+1 = easier)
Complexity (2)	0	0	-1	1	1	0	How many growing factors must be controlled? (+1 = more)
Level of Automation (4)	0	1	-1	1	1	1	(+1 = fewer human inputs required)
Growth Speed (2)	0	0	-1	1	1	-1	(+1 = faster yield rate)
Water Efficiency (3)	0	0	-1	1	1	1	(+1 = more efficient)
Energy Efficiency (3)	0	0	1	-1	0	1	(+1 = more efficient)
Spatial Efficiency (4)	0	1	-1	0	1	-1	(+1 = more space efficient)
Diversity of Crops (5)	0	-1	1	0	0	1	(+1 higher diversity of compatible crops)
Cost to Fabricate (4)	0	1	1	0	1	-1	Estimated cost to build one unit, based on required auxiliary components (+1 = cheaper)
Cost to Manufacture (1)	0	1	1	0	0	-1	Estimated cost to manufacture 50,000 units (+1 cheaper)
Maintenance Cycle (3)	0	0	0	-1	0	-1	How often is maintenance required? (+1 = less frequent)
Noise (1)	0	1	1	0	0	0	Noise generated during operation, based on auxiliary components (+1 = less noise)
Aesthetics (1)	0	1	-1	1	1	0	Modernism and newness of the system (+1 more modern)
Reliability (4)	0	0	1	-1	-1	0	How prone is system to failure? (+1 = more reliable)
Summary							
Total Score	**0**	**10**	**3**	**1**	**15**	**1**	

4.4 Fogponic Concept Refinement (EG)

Refinements to the Fogponic concept in *Figure 4* were influenced by existing Fogponic solutions. LettUs Grow's grow-bed tray architecture [13] was the foundation of the concept, however its use in industrial growing introduced misaligned design features for the project objectives. For instance, their grow-bed architecture is responsible for capturing reflux fluid for immediate re-atomisation. As plant roots absorb nutrients at different rates, reflux fluid contains an imbalanced nutrient concentration and may introduce pathogens into the water reservoir. LettUs Grow address this with a separate industrial tank for periodic filtration and sanitisation.

The inclusion of such a filtration system in a smaller, self-contained system would increase system complexity. A separate concern with the initial concept was the precise airflow control necessary to achieve uniform mist distribution throughout the shelved mist chamber geometry.

A more relevant point of inspiration was the Vext 2.0 product [14]. Similarly intended for domestic use, their Fogponic system features a vertical growing wall with a simple, rectangular mist chamber geometry. The Vext 2.0 unit is shown in *Figure 5*.

By adopting a similar geometry, the required complexity of airflow was reduced whilst improving spatial efficiency. To address the filtration challenge, the atomisation tray was offset such that the mist was blown horizontally before being blown upwards, allowing reflux condensation to fall into a filtration module immediately below. This concept is described in *Figure 6*.

A two-pronged vent was ideated to enable a single fan to fulfil the bidirectional air flow requirement. Whilst this improved the concept feasibility, the mist distribution was now reliant on the vent geometry. This presented a complex point of optimisation which, if not achieved, would lead to poor mist distribution at the top of the mist chamber. This challenge was deemed unfavourable in the allotted project timeframe

Hydroponic Tower farms [15]are a popular choice for DIY growers. Pumping nutrient solution above vertically stacked plants and allowing it to drip down through the roots and into a basin presented a simple yet effective solution. A similar approach was considered for Fogponics, whereby water is pumped into a misting tray above the roots and atomised. Gravity and a positive pressure gradient would hypothetically push the mist downwards into the mist chamber, eliminating the need for controlled air flow altogether. Whilst this solution departed from a self-contained Mist Engine unit, it elegantly addressed the engineering challenges around the previous concepts whilst improving energy efficiency by eliminating a fan from the mist chamber. This configuration is presented in the Embodiment Design section.

Figure 5 – Vext 2.0

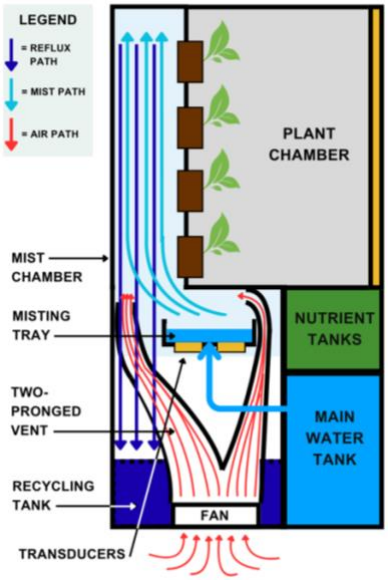

Figure 6 – Second iteration of the Fogponic concept

5 Embodiment Design

5.1 System Decomposition (EG)

Proceeding with Fogponics, the overall system was decomposed into key subsystems and their constituents, shown in *Figure 7*. Supplementary microcontroller architecture and control flowchart diagrams are detailed in *Figure 25 & 27* respectively.

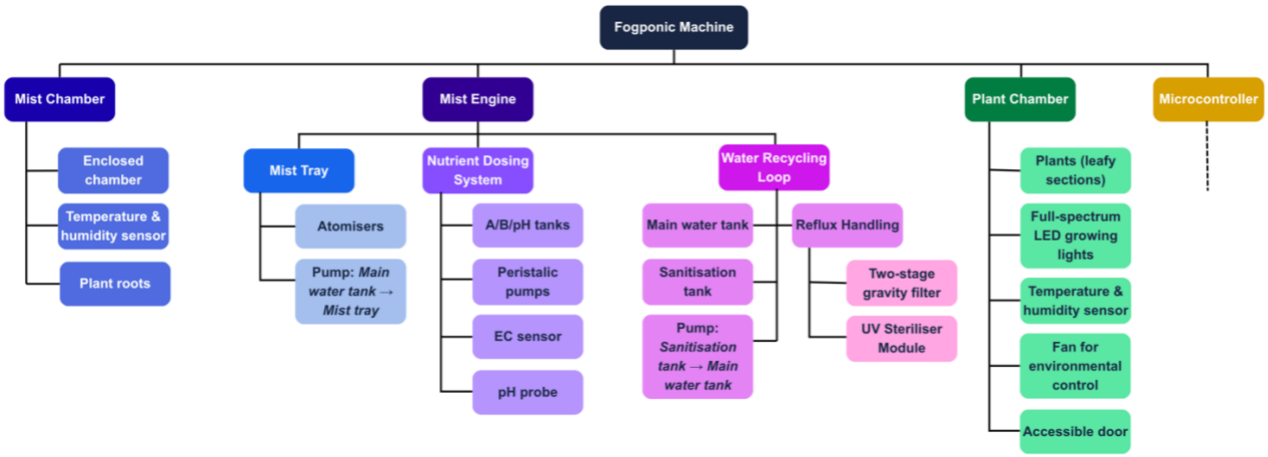

Figure 7 - System Decomposition Diagram

The bulk of the actuated components are encapsulated in the Mist Engine subsystem, responsible for mixing nutrients, mist generation and recycling the portion of reflux fluid not absorbed by plant roots.

Despite the project scope omitting all horticultural aspects from the final prototype, their inclusion in the system decomposition remained crucial to enable seamless future integration. Excluded elements include:

- All child elements of the Nutrient Dosing System
- Full-spectrum LED growing lights
- Temperature & Humidity sensor, within plant chamber
- UV Steriliser module (UV light)

Elements which take up significant physical space, whether directly or for mounting purposes, were given ample space for integration in the physical design. Wiring channels were not incorporated as their addition was unlikely to conflict with existing design features.

5.2 Overall Configuration and Features (EG)

5.2.1 Structural Requirements & Priorities

A suite of structural constraints informed the physical implementation of the described configuration. PDS requirements 1a and 1b establish the overall dimensional target and need for visual appeal. As the product is ultimately intended for domestic use, user-friendly operation and reliability were top priorities for the design. Tanks and filters benefit from being removable for ease-of-cleaning, and the physical design must enable sensor integration for monitoring and failure state logic. Where feasible, mechanical fail-safes should provide an additional passive layer of redundancy in the event of microcontroller failure. Separation of wet and dry regions was another reliability-oriented priority. This would enable targeted waterproofing where necessary.

These requirements, coupled with a short project timeframe, presented FDM 3D printing as an ideal fabrication method. The maximum build volume of the 3D printer presented a new set of structural constraints. A Bambu Lab P1S was used as the primary fabrication device, which specifies a maximum build volume of 256x256x256mm. In the interests of waterproofing critical components, i.e. the Main Water Tank, their size was constrained to this build volume. This affected the product dimensions, as crop yield to footprint ratio informed the core value proposition and took precedence over PDS requirement 1a. Non-critical components were not constrained, as silicone sealant between multi-part assemblies could achieve satisfactory watertightness.

5.2.2 Proposed Structural Architecture

The final architecture was proposed following a comprehensive synthesis of the structural constraints and design objectives. This was depicted within *Figures 8-11*. Some labels have been repeated for readability.

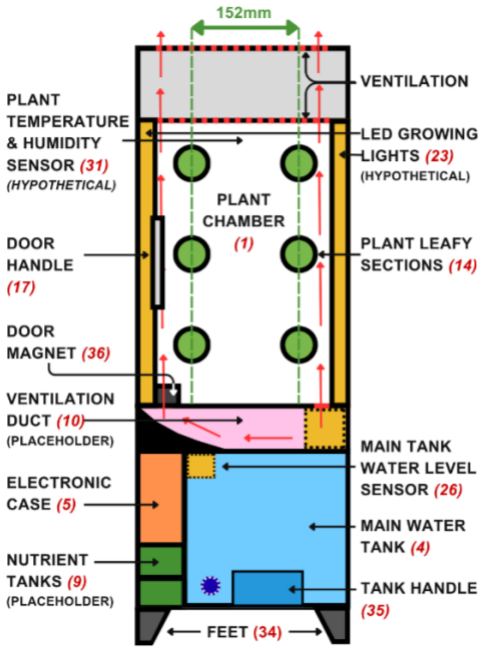

Figure 8 – Proposed Architecture: Front view

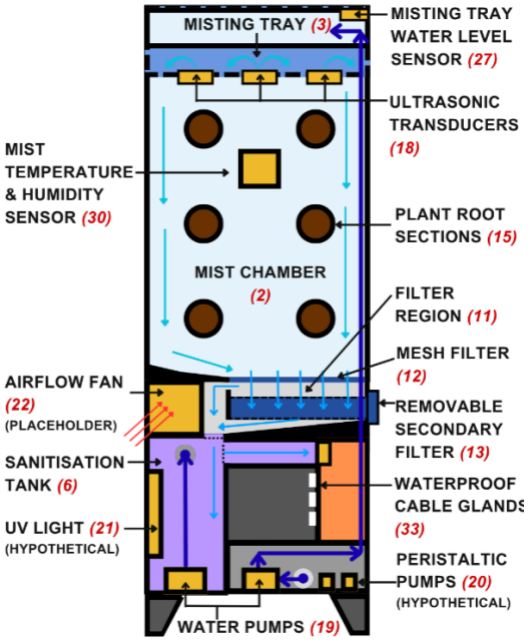

Figure 9 – Proposed Architecture: Rear view

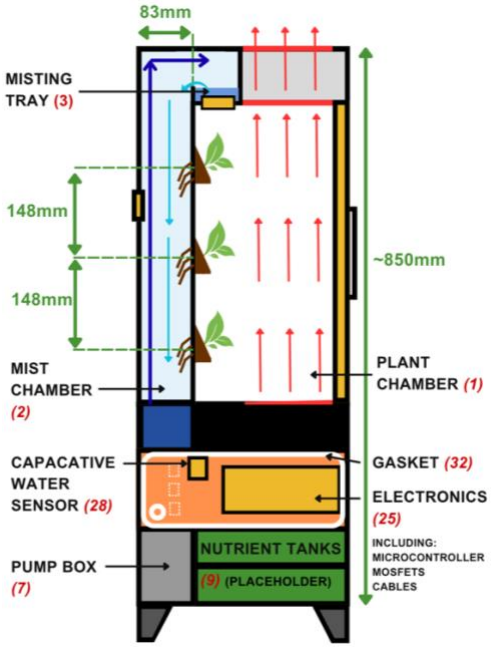

Figure 10 – Proposed Architecture: Left view

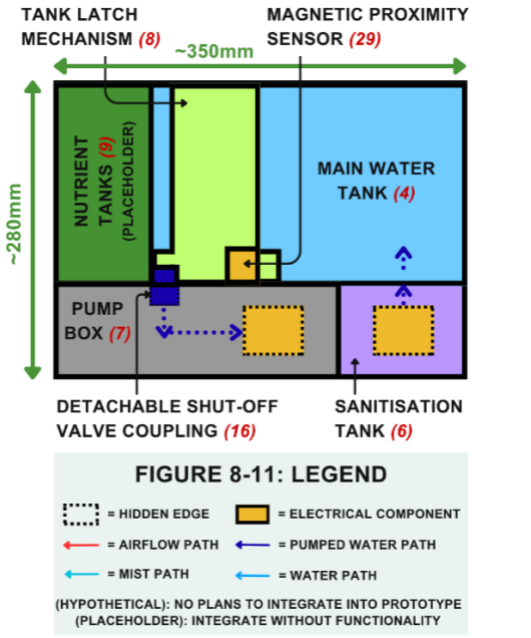

Figure 11 – Proposed Architecture: Bottom view & Legend

The external layout resembles a downsized Vext 2.0, containing just six planters compared to Vext's 27. The plant hole spacing was kept consistent as it was assumed that Vext's geometry [16]was thoroughly validated. The same reasoning informed the Mist Chamber *(2)* and Plant Chamber *(1)* depth.

The Filtration Region *(11)* comprised a two-stage filter. The first stage was a permanently fixed stainless steel Mesh Filter *(12)* of size X, intended to catch larger root debris and larger biofilm. The Removable Secondary Filter *(13)* was a drawer containing an aquarium sponge filter of a finer 20 PPI, intended to capture smaller impurities.

This architecture is explored and further justified in subsequent sections.

5.2.3 Ease-of-access, Maintenance, Modularity

The core structural layout of the design was influenced considerably by a need for accessibility. Components were assessed by how often user interactions were required to determine their ideal location

on the device. The most accessible face of the device was the front, observed in Figure 8. Either the left or right sides may be accessible. However, to allow the device to be placed in the corner of a room, only the left side was designated as accessible. The rear side will likely face the wall during routine operation. The bottom surface may be accessed without visibility, and the top surface is largely inaccessible unless the machine is placed on a low working surface.

Three levels of accessibility were defined for comparison purposes: **Routine Access**, **Maintenance Access** and **Consideration for Modularity**. As the current design was open-sourced, **Consideration for Modularity** enabled further contribution and research from the wider community. *Table 4* assesses the accessibility of relevant components and describes how they were enabled in the design.

Table 4 – Accessibility of different components

Component	Accessibility Category	Reason for Classification	Enabling Design Features
Plant Chamber *(1)*	Routine Access	Once crops are fully developed, harvesting can occur daily [17].	Positioned on the **front face**. Hinged door with handle and holding magnet. The surrounding enclosure and door were made from transparent acrylic for crop visibility.
Main Water Tank *(4)*	Routine Access	Must be removed for easy refill and occasional cleaning. Estimation by comparison to Vext 2.0 specifications indicate a 21-day minimum refill cycle [17].	Positioned on **front face**. Tank featured an integrated handle and rests on rails for reduced friction during removal and insertion. A Detachable Shut-off Valve Coupling *(14)* [18] [19] seals itself upon tank removal, preventing leaks. The Main Tank Water Level Sensor *(26)* used ToF sensing, enabling a wire-free tank that can be submerged for thorough cleaning
Tank Latch Mechanism *(8)*	Routine Access	The Detachable Shut-off Valve Coupling *(14)* requires lever actuation to release the Main Water Tank *(4)*.	Positioned on **bottom face** since operation is purely tactile. Sliding linkage mechanism allows latch handle to be situated near the front face for easy access whilst actuating the shut-off valve lever located on the rear side.
Nutrient Tanks *(9)*	Routine Access	Rough estimate based on Vext 2.0 [17] suggest a refill frequency of 4 months.	Positioned on the **front face**. Tanks are designed as removable drawers and connect to the Pump Box *(7)* with shut-off valves.
Removable Secondary Filter *(13)*	Maintenance Access	Whilst long-term filtration testing was not included in the project scope, the aquarium filter must nevertheless be periodically replaced to ensure effective particle capture	Positioned on the **left face**. An ideal front facing filter tank would require the filtration system to fill the space above the tank. Without further development and testing of filtration characteristics, over optimisation risked non-functionality. A removable drawer form factor was used.
Misting Tray *(3)*	Consideration for Modularity	The atomisation setup defines the system performance. Tray interchangeability enables further research and optimisation.	Positioned on the **top face.** Like the Main Water Tank, the Misting Tray Water Level used ToF sensing and was mounted to a lid. The tray was therefore removable without affecting surrounding components.
Electronic Case *(5)*	Consideration for Modularity	Introducing new auxiliary components may require additions to the microcontroller system.	Positioned on the **left face**. To achieve access on the same face as the Removable Secondary Filter *(13)*, the Filter Region *(11)* was staggered in relation to the Sanitisation Tank *(6)*. The Airflow Fan *(22)* was moved to occupy the dead space.
Pump Box *(7)*	Consideration for Modularity	Future incorporation of Peristaltic Pumps *(20)* and potential water pump replacement benefit from an accessible enclosure.	Positioned on the **rear face**. A recess was designed above the component, alongside a removable lid, allowing for easy access and clearance for component swapping.

5.2.4 Wet Regions, Waterproofing

The device was required to handle fluid reliably in several key regions: Main Water Tank *(4)*, Sanitisation Tank *(6)*, Misting Tray *(3)*, Filtration Region *(11)*, and **any instance where fluid must travel between these areas**. A single water pump was necessary to transport nutrient solution from the Main Water Tank upwards to the Misting Tray. Passive gravity-feeding was considered where feasible, as it improved energy efficiency. This rationale was applied in the inclusion of a gravity-fed Filter Region *(11)*.

The filtered fluid path can be seen in Figure 9. The choice to include a dedicated Sanitisation Tank was driven by the functional characteristics of UV sanitisation. A manufacturer-specified period of UV exposure was required to guarantee acceptable sterilisation. A pump positioned at the base of this tank allowed for older fluid to be removed, whilst new fluid entered at the top. This fluid was pumped back into the Main Water Tank.

Lastly, fluid from the Misting Tray reached the Filtration System via atomisation and condensation. This region therefore required vapour containment instead of watertightness. All aforementioned wet regions and measured taken for fluid containment were summarised in *Table 5*.

Table 5 – Wet regions

Wet Region	Extent of Fluid Exposure	Measures Taken	Rationale
Main Water Tank *(4)*	Must contain 8L of water	Single PETG HF* print. O-ring + silicone glue for shut-off valve	Shut-off valve was located at tank floor, exposed to 1.67 kPa of hydrostatic pressure. O-ring was required, silicone as precautionary measure
Sanitisation Tank *(6)*	Must contain 1.5L of water	Single PETG HF* print	PETG HF's* high melt index and low saturated water absorption rate produced sufficiently watertight prints (for low pressure applications)
Misting Tray *(3)*	Must contain 1L of water	Single PETG HF* print. O-rings for screw holes	Same reasoning as above. O-rings for screw holes designed to extend through the container walls.
Filtration Region *(11)*	Exposed to low flow rate of condensed reflux	Multiple PETG HF* prints joined with clear epoxy at tongue & groove joints. Surface edge brushed with silicone glue	Assuming 80% of atomised water (worse case) is recycled, the resulting flow rate is a low 280ml/hr. Tongue & groove joints create a tougher escape path for liquid, silicone glue as precaution.
Main Water Tank *(4)* → Misting Tray *(3)*	Pumped water	Silicone tube with undersized inner diameter	The potential leak points were the interface between tube and pump/valve. Undersized inner diameter ensures sufficient rubber deformation.
Misting Tray *(3)* → Filtration Region *(11)*	Exposed to dense mist & condensation runoff	Multiple PETG HF* prints joined with clear epoxy at tongue & groove joints. Surface edge brushed with silicone glue	Same rationale as Filtration Region.
Filtration Region *(11)* → Sanitisation Tank *(6)*	Gravity assisted water path, dense mist	Single PETG* HF print. Drawer module designed to not intersect with the liquid path. Drawer was gasketed	Filter drawer was designed for frequent user-interaction. Gasket ensured good seal against potential mist escape and precautionary measure against liquid.
Sanitisation Tank *(6)* → Main Water Tank *(4)*	Pumped water	Silicone tube with undersized inner diameter	Same rationale as Main Water Tank → Misting Tray
*Bambu Lab's PETG High Flow filament			

Whilst wet zones were designed for reliable containment during normal operation, certain edge cases informed additional **physical** safety measures. If the user neglected to replace/clean the Secondary Filter *(13)*, it was possible that the fluid path would become impeded by waste particles. This would risk fluid pooling upwards into the Mist Chamber *(2)*, which was not specified to handle liquid of any considerable depth. Therefore, an alternate fluid channel was incorporated into the Filter Region *(11)*, shown by the L shaped arrow. Fluid will bypass the filter in these cases, avoiding catastrophic failure.

It was reasonable to assume occasional splashes from routine tank filling. And whilst not anticipated, leaks may also arise between wet regions due to poor tolerancing or incorrect assembly. This necessitated a precautionary effort into waterproofing the Electronic Case *(5)*. The main enclosure was sized to print in a single PETG HF piece. To incorporate wiring without compromising on a seal, wall-mounted Waterproof Cable Glands *(33)* were used. A recessed Gasket *(32)* was incorporated into the main enclosure to interface with a PETG HF lid component, fixed with corner screws.

5.2.5 Fabrication Strategy

FDM 3D printing was chosen as the primary fabrication method. *Table 6* demonstrates the rationale behind material selection amongst several contending filament types. Low price and high print speed allow for rapid iteration, whilst water absorption rate and melt index partially characterise the watertightness of resulting prints. Only Bambu Lab's range of filament was considered for fabrication, as third-party filaments presented a higher risk of failure without fine-tuned print settings.

Table 6: Material Selection

Candidate Filament	Price (£/kg)	Max print speed (mm^3/s)	Saturated Water Absorption Rate (%)	Melt Index (g/10 min)	Additional comments
PETG Basic [20]	10.25	200	0.10	22.9 ± 2.4	Highly hydrolytically stable
PETG HF [21]	10.25	300	0.40	28.2 ± 2.7	Similar hydrolytic stability. Dimensional accuracy is improved with reduced oozing.
PETG-CF [22]	28.99	200	0.30	19.3 ± 2.4	Fibre-reinforced filament is known to shed microscopic fibres [23]. Unsuitable for food safety
ABS [24]	10.25	250	0.65	34.2 ± 3.8	Acetone vapour smoothing can be used to reduce surface porosity. Although high thermal contraction increases the risk of layer delamination, potentially causing leaks
PC [25]	36.99	200	0.25	32.2 ± 2.9	Even higher thermal contraction than ABS. Challenging to print large parts without significant warping

PETG HF and ABS exhibited the greatest affinity for the project requirements. Their high melt index helps to reduce the size of internal void fractions, improving their reliability as water vessels. Although the challenges around ABS warping, especially in larger prints, presented PETG HF as the clear winner.

To fulfil PDS requirement 1b: "blend with the decoration of the household", an outer façade was integrated into the design. The need for visual integration with other household furniture presented Wood PLA as an ideal material. A textured surface was introduced to the external-facing surface by printing onto a textured PEI build plate. To enable observation of mist generation and the reflux fluid path shown in *Figure 9* (for testing purposes), PETG Translucent was used. Translucency was incorporated into the Sanitisation Tank *(6),* Filter Region *(11)* and Mist Chamber *(6)*, although subsequent attempts during prototyping outlined the difficulties of achieving optical clearness. A window into the Mist Chamber *(6)*, originally designed in PETG Translucent, was ultimately replaced with a sheet of clear acrylic.

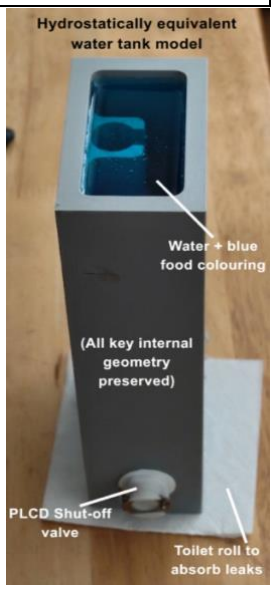

Figure 12 – Validation of PETG HF watertightness with basic print settings: Test set-up

Bricklayering [26] was explored in early prototyping to improve print watertightness. A custom post-processing script [27] caused a 'blob of death' failure on the first attempt. Diagnosing the problem uncovered the innate risk of toolhead collision with the print. Proceeding with standard settings validated complete watertightness in a hydrostatically equivalent Main Water Tank *(4)* model, test results shown in Figure (12-13). Further attempts at implementing bricklayering were not made, although material efficiency may be improved with its successful utilisation.

A 0.4mm hardened steel nozzle was chosen for an ideal balance of strength and material efficiency. Layer height was kept at the standard 0.2mm. Components with higher waterproofing specifications were printed with 6 wall loops, opposed to the standard 2. Larger components, including the Main Water Tank *(4)* and Electronic Case *(5)* used 25% infill density, whilst smaller, non-load-bearing components used 15% density. Gyroid was the preferred infill pattern, with exceptions including lids intended to clamp onto gaskets, and translucent components. The former used a triangular infill for higher in-plane rigidity, and the latter were printed with aligned rectilinear infill in attempts to enhance visibility.

Figure 13 – Validation of PETG HF watertightness with basic print settings: Test outcome

Print orientation was considered during component design. Emphasis was placed on exploiting in-plane strength whilst minimising load applications that stress the z-direction. Overhangs were avoided where feasible, although this was a secondary priority. Optimal tolerancing was determined through a series of targeted test prints, depicted in Figures (14-16). Tongue and groove joints required definitive validation before full production. Other interference joints and looser fits, including drawer holders, were similarly validated. The explored range of tolerances included ±0.1mm, ±0.15mm, ±0.2mm and ±0.3mm. ±0.2mm was found to work universally for interference joints, and ±0.3mm was suitable for looser fits.

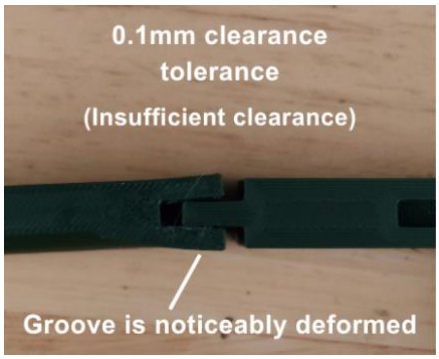

Figure 14 – Tongue & groove joint, 0.1mm clearance

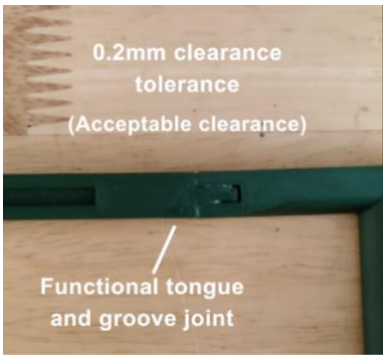

Figure 15 – Tongue & groove joint, 0.2mm clearance

Figure 16 – Drawer, top 0.2mm clearance, bottom 0.3mm clearance

Interference joints bonded by clear epoxy were employed in permanent assemblies, notably the Mist Chamber *(2)*. To enable accessibility, screws and heat-set brass inserts were used in semi-permanent assemblies. Countersunk screws were preferred for their improved spatial efficiency.

The spatial gains afforded by the complex geometry of designed components did not always present a strong interface to fasten bodies. Therefore, the design benefited from a rigid frame constructed from 20mm T-slot aluminium profiles. Components were instead fastened to the T-slots. This approach eliminated the need for a robust FEA analysis, as it was assumed that any loads experienced during routine operation and machine transportation would be well within the safety margin.

5.3 Atomiser Design (FM)

5.3.1 Objectives

The primary objective of this section is to identify, select, and validate an ultrasonic atomization module capable of generating the precise mist required for a fogponics system. To achieve this, the following methodology has been used:

1) Research: Conduct background research into the physical principles and mathematical modelling of ultrasonic mist generation to understand how operating frequency controls droplet size;
2) Procurement: Select and purchase commercially available ultrasonic components that theoretically align with the required constraints;
3) Physical testing: Design and conduct physical tests across multiple configurations to evaluate real-world mist generation capabilities;
4) Analysis: Analyse the results of the physical tests.

Although the initial prototype operates with pure water, the atomizer was initially engineered to work efficiently with nutrients, ensuring future iterations will require minimal mechanical modifications.

5.3.2 Mathematical Modelling

Atomization depends on the excitation frequency of the transducer (f), where higher operating frequencies produce a more concentrated and finer droplets, while lower frequencies produce larger droplets [28].

Initial mathematical modelling considered a comprehensive correlation that included a continuous flow rate variable (Q). However, for simplicity of calculations and overall system feasibility, it was decided that the designed prototype would operate without a continuous flow of new water pumped directly across the atomizing surface. Once the tank where mist is being produce is filled, the water volume is considered to be stagnant, resulting in a net continuous flow rate of zero (Q = 0). While the ultrasonic vibrations induce localised fluid movement, no new liquid is actively added to or removed from the working system, consequently, the flow rate parameter can be safely eliminated, and the droplet size (d_p) calculation simplifies to Lang's correlation:

$$d_p = 0.34 \cdot \left(\frac{8 \cdot \pi \cdot \sigma}{\rho \cdot f^2}\right)^{0.333} \quad (1)$$

Where σ is surface tension of water, ρ is liquid density, f is excitation frequency. Rearranging Equation 1, the target frequency can be calculated as:

$$f = \sqrt{\frac{8 \cdot \pi \cdot \sigma \cdot 0.34^3}{\rho \cdot d_p^3}} \quad (2)$$

Where $\sigma = 0.0728\ \mathrm{kg/s^2}$ [29], $\rho = 998.2\ \mathrm{kg/m^3}$ [30] if water is assumed to be at 20°C. d_p is the droplet size in meters.

5.3.3 Droplet Size Requirement

To obtain the most efficient system, a very specific droplet size must be obtained. Research establishes that the optimal range for droplet size in fogponics systems is typically between 5 and 30 $\mu\mathrm{m}$. Aiming for the higher end of the spectrum, specifically around 30 $\mu\mathrm{m}$, was determined to be the best approach. This targeted size was selected because when nutrients are mixed with water, liquid salts are added to the solution, and if it is too strong, it can damage root cells. Larger droplets act as a buffer, diluting the impact of the salts on the root surface and helping to physically remove previous salt build-ups. Furthermore, larger droplets allow roots to develop stronger and thicker, making them more resilient to chemical stress, whereas fine fog causes roots to grow extremely dense and delicate [31].

Assuming a target droplet size of 30 $\mu\mathrm{m}$, the theoretical frequency calculated using *Equation 2* is 51kHz, which prompted the initial selection of a piezoelectric transducer around 50kHz.

5.3.4 Commercially available options

A piezoelectric transducer operates by converting electrical energy into high-frequency mechanical vibrations. When an electrical signal is applied, the ultrasonic surface physically moves and vibrates in order to break the liquid into droplets [32]. To determine the best component for the prototype, two commercially available options were initially evaluated against the optimal 30-micrometer droplet requirement, as summarised in *Table 7*.

Table 7 - Commercially available options for mist generation

Component type	Operating frequency	Droplet size	Evaluations and Limitations
Household humidifier atomizer [33]	1.7 MHz	2.9 μm	• Very fine water droplets production • Guaranteed mist generation
Atomization module [34]	105 kHz	18.8 μm	• Easy integration with microcontroller • Operating at only 2W, it limits the amount of mist it can generate

While the 105 kHz atomization module was discarded because of low mist generation, the 1.7 MHz humidifiers' atomizers were initially considered as they provide a basic benchmark for fog production.

However, to overcome these limitations and achieve both the required droplet size and the high volume of mist necessary for a functioning fogponics chamber, initial physical testing was directed toward higher-power, low-frequency piezoelectric transducers.

5.3.5 Transducer Selection and Initial Prototyping

Industrial transducers are mass-produced at standard frequencies of 28kHz, which using *Equation 5* gives a droplet size of 45 μm, or 40kHz, which generates 36 μm droplets (closer to the 30 μm ideal size). While these transducers are primarily for ultrasonic cleaning applications, custom manufacturing a specific 50kHz transducer was not feasible for the initial prototyping phase due to budget and project timeline constraints. Consequently, when initiating physical testing, two different types of commercially available 40kHz piezoelectric transducers were evaluated: a 35W ceramic sheet disc format (*Figure 17*), and a 60W cylindrical format (*Figure 18*). While both operate at the required frequency to theoretically produce the target 36 μm droplets, the cylindrical component was selected for testing due to significant practical advantages.

Figure 17 - Ceramic disc transducer

Figure 18 - Cylindrical transducer

Manual wiring is a primary requirement for this project phase. The bare ceramic disc features extremely thin silver electrodes that are highly sensitive to heat. Manual soldering would carry a high risk of melting this coating, which would permanently damage the component. In contrast, the cylindrical transducer is equipped with large, robust metal tabs. These dedicated connection points ensure a reliable electrical joint while minimising the risk of component failure during assembly.

Furthermore, the power rating difference between the two components influenced the selection. In ultrasonic atomization, while frequency controls the droplet size, wattage dictates the amplitude of the vibration [35]. To break a liquid into droplets, a transducer must reach a threshold amplitude, and the higher power of the 60W cylinder results in the component being more likely to pass the critical threshold.

5.3.6 Testing

To evaluate the atomization capabilities of the 40kHz transducer across different physical configurations. A signal generator was used to produce the required frequency, while an amplifier was used to reach high operating voltages. All the variable considered in this section have been summarised in *Table 8*.

Table 8 - Summary of variables considered in the testing phase

Variable Type	Parameter	Value	Rationale
Constant variables	Operating frequency	40 kHz	Set by a signal generator to match the theoretical requirement
	Signal amplitude	600mV ($\mathrm{mV_{PP}}$)	Standard input generated prior to amplification
	Operating voltage	100 V	Maximum operating voltage of atomizer, reached using amplifier
	Fluid Composition	Pure tap water	Prevents mineral density changes
	Water temperature	20°C	Maintains constant fluid density (ρ) and surface tension (σ)
Independent Variables	Submersion depth	Varied across tests	To identify optimal depth to break water's surface tension
	Mounting configuration	- Direct submersion (Figure 19); - 10mm-thick baking tray (Figure 20); - 1mm-thick stainless-steel plate (Figure 21).	To observe how different transmission mediums and dampening effects impact energy transfer
Dependent Variables	Mist generation	Observation	Primary success metric to determine if fluid atomization was achieved
	Surface agitation	Qualitative observation	Secondary metric to confirm acoustic resonance

The initial testing phase involved submerging the transducer directly into the water reservoir, as shown in Figure 19. This configuration was selected first to prevent the acoustic energy dissipation that occurs when vibrations are transmitted through a medium, such as a metal plate. By maximising the direct transfer of kinetic energy into water, this approach theoretically offered the highest probability of generating mist.

To ensure electrical safety and prevent short circuits, a custom 3D-printed tank was utilised, and silicone was applied to seal the components without dampening the vibrations. Upon activation this, this configuration failed to produce any mist. Even though different water levels were tested, no visible difference was achieved.

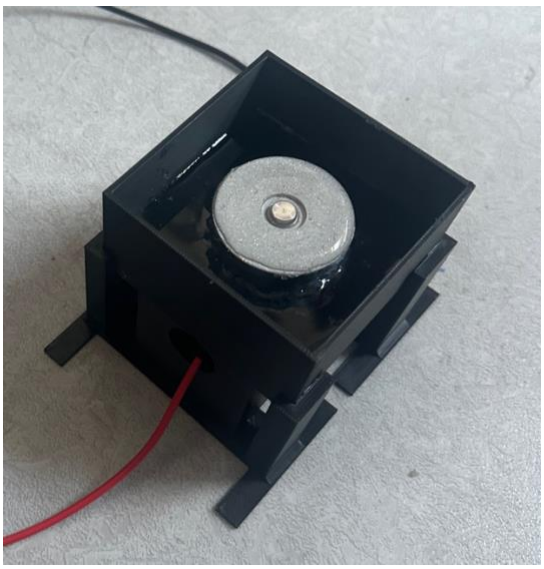

Figure 19 - Transducer submerged in water tank

Industrial 40kHz cleaning transducer are specifically manufactured to be bonded to the bottom of a metal plate, rather than being directly submerged. To replicate this operating condition, a second test was conducted. The transducer was therefore bonded to the underside of a standard metal baking tray using high-strength epoxy adhesive, as shown in *Figure 20*. When the transducer was powered, the system successfully reached a resonance point, indicated by intense agitation of the water directly above the component, however, the system failed to achieve atomization. This failure was attributed to the material properties and geometry of the baking tray. The relatively thick, and flexible metal of the tray acted as a mechanical dampener, absorbing a portion of the ultrasonic energy. Furthermore, the solid walls of the tray likely dissipated a significant amount of power.

Figure 20 - Transducer glued to metal tray

To resolve the dampening and dissipation issues observed in the second test, a third configuration was designed. This setup utilised a flat, stainless-steel plate with side walls made of silicone, as shown in *Figure 21*. Silicone was specifically chosen because it provides a reliable watertight seal while mechanically decoupling the side walls of the tank. Stainless-steel was selected because it is the industry standard for ultrasonic transmission as it possesses high density and excellent acoustic stiffness [36].

The plate thickness was chosen to be 1mm because it represents the lower limit for standard ultrasonic cleaning tanks [37]. This dimension minimises mechanical dampening while providing sufficient structural toughness to prevent metal fatigue and tearing during testing.

The overall planar dimensions of 100x50mm were established to balance fluid capacity with minimal structural weight. The diameter of the chosen 40kHz transducer is 44mm, making the 50mm width enough

to provide the necessary clearance around the transducer. The 100mm length provides an adequate surface area to contain water, without adding excessive mass to the vibrating structure.

Figure 21 - 3rd setup before transducer was powered

Figure 22 - 3rd setup when transducer was generating 40kHz frequency

Despite the optimisations made in the third configuration, the setup ultimately failed to generate mist. While a noticeably more intense agitation of the water surface was observed compared to the second test, indicating improved acoustic transmission through the thinner 1mm plate, fluid atomisation was not achieved.

Post-testing analysis revealed that this failure was caused by the selected transducer. The initial choice of the 60W cylindrical transducer was driven by its high electrical power rating, under the assumption that higher wattage would guarantee superior atomization. However, this assumption, proved to be a critical mechanical oversight.

5.3.7 Analysis of Results

In acoustic engineering, mechanical work is a combination of force and amplitude. The cylindrical transducer is engineered with heavy steel and aluminium blocks to generate massive force, allowing it to push against thick industrial tanks. Because so much energy is consumed generating this force, the resulting physical displacement (amplitude) is extremely low. Fluid atomization, however, requires high-speed, high-amplitude surface vibrations to rapidly break the water surface tension.

Consequently, a standard disc-like piezoelectric transducer (*Figure 17*) would have been the correct mechanical choice. Unlike the cylindrical model, a bare ceramic disc lacks the massive metal end-blocks. Without having to push a heavy mechanical load, the disc transmits its electrical power directly into high-amplitude kinetic energy. Even at a significantly lower power rating (35W compared to 60W) than the chosen option, the bare disc would likely achieve the rapid flexural displacement required to generate mist.

Because this mechanical limitation was only discovered after the component testing phase was completed, primary testing of the assembled fogponics system will be conducted using a standard, commercially available 1.7MHz ultrasonic mist maker, shown in *Figure 23*. Before implementing it in the final assembly, its functionality has been tested, and, as shown in *Figure 24*, it instantly produced a dense and continuous mist.

Figure 23 - Mist maker setup

Figure 24 - Mist maker when activated

While the 1.7MHz module produces droplets finer than 30 μm, it is acceptable for the initial prototype because the system will operate using only water. However, for future commercial developments that fully integrate nutrient solutions, the atomization module must be upgraded to a low-frequency (40kHz), high-amplitude bare ceramic disc transducer.

5.4 Sensor and Components Selection (PM)

5.4.1 Context and Research

Sensors and auxiliary components were selected to detect the main hydraulic, containment, and docking faults and also support warning messages, prevent operation under unsafe conditions, or shut down pumps and actuators while keeping electronics separated from the wet fluid-handling area. Since roots in fogponics have little stored water around them, interruptions to circulation or misting can affect plant health quickly, making component selection a systems-level task in which sensing, protection, actuation, and physical layout had to work together.

The monitored risks, summarised in *Table 6*, were selected based on failure severity and how quick each fault could become harmful. Each addresses a fault mode that could cause rapid plant loss, water leakage, equipment damage, or unsafe operation if not detected early. Selection therefore focused on components that could limit damage by detecting faults early and shutting down pumps or actuators where necessary, while remaining practical to build, test, clean, and maintain. Preference was given to components with clear manufacturer data, Arduino compatibility, short lead times, available libraries, wiring examples, and supplier documentation. This reduced development risk for a first prototype.

Components were also selected based on nominal function, suitability for a humid and splash-prone enclosure, compatibility with the Arduino-based control architecture, circuitry requirements, maintenance burden, and ease of future testing. [38]

pH and Electrical conductivity (EC) sensing require calibrated probes, additional circuitry, and a calibration procedure that was beyond the scope and available integration time of this first prototype. Nutrient flow sensing would require inline sensors that complicate wet-zone layout and cleaning. Dedicated mist-output sensing and water-temperature sensing were excluded to limit first-prototype complexity. Chamber humidity was used only as a broad indication of misting and was not treated as proof of root-zone wetting. These remain possible additions once the basic water-delivery system, tray control logic, and fault-detection approach have been proven reliable.

5.4.2 Selection Criteria

Table 9 combines the sensing and actuation requirements, selected components, and what still needs to be tested before the component can be treated as fully proven. The monitored faults correspond to the protective states used in the microcontroller fault-handling logic in Section 5.5.7. Components listed as future provisions were physically or electrically allowed for in the design but were not required for the prototype to operated. Detailed decisions on actuator drivers, power switching, and microcontroller connections are covered separately in Section 5.5. Where component suitability could not be proven from datasheet information alone, the remaining validation need was treated as a test requirement rather than assumed performance.

Table 9 – Component selection matrix -

Subsystem	Requirement / fault addressed	Selected component	Key selection rationale	Key limitation / validation need
Reservoir and tray level sensing	Detect low reservoir level before the pump inlet can draw air and provide indication if tray water level is too low or too high.	VL53L1X time-of-flight sensors	Continuous water level monitoring without wetted electrodes or mechanical floats.	Reservoir warning/shutdown levels must be set before the pump inlet can draw air. The tray sensor is only a backup indication for obvious low/high water levels, not a precise atomiser-depth control sensor.
Chamber temperature and Relative humidity (RH)	Monitor chamber temperature and RH during misting	SHT85 specified; DHT11 used in prototype	SHT85 selected for more accurate humidity/temperature monitoring in a humid chamber. DHT11 used as a short-term substitute.	SHT85 can't be placed directly under mist path and was relatively expensive. DHT11 is only suitable for rough humidity trends, not calibrated humidity control.
Leak detection	Detect leaked water once it reaches the designed leak pocket.	DFRobot SEN0508 capacitive liquid detector	Detects liquid through a non-conductive wall, keeping the sensor outside the wet region.	Only detects leaks directed into the leak pocket; enclosure geometry must guide liquid to the sensing region.
Tank presence / docking proximity	Detect whether the removable tank is inserted correctly before operation	RS PRO magnetic proximity sensor	Avoids a mechanical switch contact at a frequently handled, splash-prone docking interface.	Detects magnet proximity only; it does not prove full tank alignment or hydraulic sealing. Mechanical locating features are still required.
Feed and return circulation	Transfer nutrient solution between reservoir and tray at 0.8 m lift	Two Whadda WPM421 brushless DC pumps	Compact, low-power pump selected for required lift height, wet-zone suitability, and automated water-transfer applications.	Not self-priming, so inlet must remain flooded. Installed flow rate, tray water-level stability, pump start-up current, and feed/return duty cycles require validation.
Plant-chamber air movement provision	Provide future option for chamber airflow or temperature control	AF80-00136 AxiForce axial fan provision; not used in current prototype	Retained from an earlier concept where the fan was intended to move mist upwards through the chamber	Oversized for continuous domestic use and electrically demanding; future use requires re-sizing, separate power/driver validation, and EMI/start-up current checks.
I2C address management	Allow both identical level sensors to communicate with the microcontroller	TCA9548A multiplexer	Resolves the fixed I2C address conflict between both VL53L1X sensors.	Adds another interface device that must be configured and validated.

5.4.3 Water Level Sensing and Pump Protection

Reservoir water level sensing protects against pump dry-running, while tray water level monitoring provides backup indication of obviously low or high-water level around the atomiser. The VL53L1X was selected because it provides digital level indication without wetted electrodes or mechanical floats, reducing fouling, wear, and cleaning complexity compared with conductive probes or float switches. Its minimum sensing distance of approximately 40 mm and typical ±25 mm accuracy made it suitable for detecting large reservoir-level changes, such as normal, warning, and shutdown regions. [39]

The PDS required low-reservoir detection at 20% tank capacity, but pump protection depends on the actual water height at the pump inlet, not only on percentage tank volume. The warning and shutdown thresholds should therefore be set using the measured water level at which the pump inlet would first begin to draw air. The shutdown threshold should trigger before this point, with allowance for sensor error, water-surface movement, and hysteresis. This is important because the selected pumps are not self-priming; if the inlet draws air, the pump may lose prime and circulation may not restart reliably even if the reservoir is refilled.

The tray application is more demanding than the reservoir because the atomiser operating-depth range is shallow. The VL53L1X was selected before the final atomiser had been chosen, so the required tray water depth was not fully known at the point of sensor selection. Once the atomiser was selected, its 40 mm maximum water level made the VL53L1X less suitable for this location because the sensor's typical ±25 mm uncertainty is large relative to the allowable tray-depth range.

The tray sensor was therefore retained as a prototype compromise rather than a precision control device. Because the tray VL53L1X cannot measure the narrow atomiser water-depth range accurately enough, tray protection should not rely on this sensor alone. In the current prototype, tray level should be governed primarily through conservative feed/return pump timing based on tray geometry and the atomiser water-depth limit. This is supported by extra tray height above the normal water level and an overflow/return path that directs excess water back toward the reservoir. The VL53L1X is retained only as a backup indication if the tray remains clearly too low or too high for several readings. It should not be treated as proof that the tray is operating at the correct atomiser depth or that the root zone is being wetted.

In a future iteration, tray-level sensing should be selected only after the atomiser operating-depth range and required warning/shutdown thresholds have been defined. A better choice would be a sensor with uncertainty significantly smaller than the allowable tray-depth band, such as an external capacitive level sensor through the tray wall, a pressure-based level sensor with an isolated or cleanable pressure port, or discrete high/low level switches if only protective shutdown thresholds are required.

5.4.4 I2C bus management

Both VL53L1X sensors share the same default I2C address, so a TCA9548A multiplexer was used to place them on separate I2C channels. Without the multiplexer, both identical level sensors could not be used reliably on the same bus without changing the sensing approach or adding a software workaround.

5.4.5 Leak, tank presence, and humidity Sensing

The SEN0508 was selected for leak detection because it detects liquid through a non-conductive wall up to 5 mm thick. This keeps the sensing element outside the wet region and reduces contamination, corrosion, and cleaning risk compared with exposed conductive leak probes. The SEN0508 is therefore not a standalone leak solution as it only works effectively if the enclosure geometry directs escaped liquid into the defined leak pocket, i.e. a low collection area designed to collect escaped water. [40]

The magnetic proximity sensor provides a tank-presence interlock by detecting the tank-mounted magnet. It was preferred to a microswitch because the removable tank is a frequently handled, splash-prone interface, and magnetic sensing avoids a physically pressed contact at the docking boundary. Its 14 mm sensing range provides tolerance to small placement variations, but it does not prove full tank alignment or that the water connection is sealed and leak-free, so mechanical locating features are still required. [41]

The SHT85 represents the intended design choice, while the DHT11 was only a short-term prototype substitute for rough humidity trends. Environmental sensing was included to monitor chamber conditions and help interpret condensation around optical sensors and internal surfaces. The SHT85's 0-100% RH range, ±1.5% RH accuracy, ±0.1°C temperature accuracy, and IP67 PTFE-protected membrane made it better suited to long-duration humid chamber monitoring than the DHT11, which has typical ±5% RH and ±2°C accuracy and no moisture-protected package. Even with the protected membrane, the SHT85 should be positioned away from direct mist impingement while still sampling air representative of the chamber condition. [42]

5.4.6 Pumps

Two Whadda WPM421 brushless DC pumps were selected to provide independent feed and return transfer between the reservoir and atomiser tray. This allows the tray to be filled and drained under microcontroller control but creates a risk of tray-level drift if installed feed and return flow rates differ. Pump duty cycles should therefore be tuned against measured tray behaviour rather than fixed timings alone. [43]

The pump was selected for water tray transfer and refilling the tray after the water level has fallen, rather than continuous high-flow circulation. Ideally, the required flow would be defined as:

$$Q_{required} = \frac{\Delta V_{tray}}{t_{fill}} \tag{3}$$

where $Q_{required}$ is the required pump flow rate, ΔV_{tray} is the volume of liquid needed to move the tray from low level to the intended atomiser operating water level., and t_{fill} is the acceptable refill time.

This requirement could not be fixed during component selection because the tray geometry, tubing layout, and feed/return duty cycle were still being developed. The pump was therefore screened against static lift, rough estimated flow at the required lift, electrical integration, wet-zone suitability, and the reservoir-to-tray transfer duty.

The main known hydraulic requirement was lifting nutrient solution approximately 0.8 m from the reservoir to the tray. The WPM421 has a rated maximum static lift of 3.0 m, so the required lift used approximately 26.7% of the rated maximum head:

$$\frac{H_{\text{required}}}{H_{\max}} = \frac{0.8}{3.0} = 0.267 \tag{4}$$

where H_{required} is the required vertical lift from the reservoir to the tray, and $H_{\max}$ is the pump's rated maximum static lift.

This indicated that the required lift was well below the pump's rated maximum lift. As a first-order screening estimate, assuming a linear reduction from 240 L/h at zero head to zero flow at 3.0 m head, the flow at 0.8 m would be approximately:

$$Q_{\text{est}} = Q_{\max}\left(1 - \frac{H_{\text{required}}}{H_{\max}}\right) \tag{5}$$

where Q_{est} is the estimated pump flow rate at the required lift, $Q_{\max}$ is the rated maximum pump flow at zero head, $H_{\text{required}}$is the required vertical lift, and $H_{\max}$ is the pump's rated maximum static lift.

Substituting the pump and system values gives:

$$Q_{\text{est}} = 240\left(1 - \frac{0.8}{3.0}\right) \approx 176.0 \text{ L/h} \tag{6}$$

This supported the pump selection for intermittent tray transfer, but it remains a simplified screening calculation because it does not include tubing friction, bends, fittings, restrictions, or the true pump curve. The pump still needs to be checked in the built system by measuring the actual flow rate through the final tubing and confirming that the tray level remains stable.

The WPM421 also met the prototype's practical constraints: 5-12 V DC operation, 0.35 A nominal current at 12 V, 4.2 W power demand, IP68 rating, brushless motor, compact size, and stated noise below 40 dB. More complex pump types, such as peristaltic or diaphragm pumps, were not necessary for the first prototype because the required duty was simple intermittent transfer rather than accurate metered dosing or high-pressure spraying. Because the pump is not self-priming, its inlet must remain flooded, directly supporting the need for reservoir low-level sensing and shutdown logic.

5.4.7 Future fan provision

The AF80-00136 AxiForce axial fan was originally purchased for an earlier concept in which mist was expected to be blown upwards and circulated around the chamber by the fan. The final concept uses downward mist delivery, so the fan was not required for current prototype operation. [44]

Space and wiring allowance were retained as future prototypes may require plant chamber airflow to mitigate heat from integrated lights or condensation control. However, the fan is likely oversized for continuous domestic use. Its 103 CFM airflow, 26 W power draw, 13,200 rpm speed, high start-up current, and 71 dB(A) noise rating indicate that a future design should be re-sized around measured heat load, condensation control needs, acceptable noise, and driver requirements.

Electrically, the fan would draw approximately 2.2 A at 12 V before start-up current, so it could not be powered or driven directly from the Arduino. Future use would require a separate 12 V supply path, suitable driver hardware, a shared signal ground between the Arduino and driver, decoupling, and checks for start-up current, voltage sag, EMI, and driver heating.

5.4.8 Integration and remaining validation

The component layout follows a wet-zone/dry-zone separation strategy. The reservoir, tray, misting chamber, pumps, leak detection region, and exposed sensing paths are in or near the wet fluid-handling zone, while the Arduino, multiplexer, MOSFET driver, and power distribution electronics are in a protected dry zone. Low-voltage sensor wiring should be routed separately from higher-current 12 V actuator wiring where practical.

Figures 8-11 and 28 show the physical and electrical integration of the selected components, including sensor positions, actuator locations, pump inlet height, reservoir warning/shutdown regions, leak-pocket location, wet/dry-zone separation, and separation of sensor wiring from 12 V actuator wiring.

The main unresolved uncertainties are installed pump flow, tray-level stability, atomiser mist output and overheating risk at low water level, pump start-up current, leak-pocket repeatability, and whether future airflow is required under integrated lighting. Correct reservoir level, tray level, and tank docking do not by themselves prove that the atomiser is producing mist or that mist is reaching the root zone. Atomiser function therefore remains a validation requirement and should be assessed through direct observation, whether chamber humidity rises when misting is active, and root-zone wetting checks.

Several component choices also imposed layout requirements; the non-self-priming pumps require flooded inlets, the leak sensor requires escaped liquid to be guided to a defined leak pocket, and the optical level sensors require protected sight paths and sufficient stand-off distance. The main benefit of the selection process is that the remaining weaknesses can be tested directly rather than remaining hidden. For example, pump priming can be checked by confirming that the inlet remains submerged, level-sensor false readings can be managed through mounting and temporal filtering, leaks can be tested to confirm they consistently reach the leak pocket, and tray water-level stability can be assessed through feed/return duty-cycle testing

5.5 Microcontroller and Programming (EC)

This section describes the design and implementation of the microcontroller system used to control the aeroponics machine. It outlines the system requirements, overall architecture, and justification for the selection of the Arduino Uno R4 Wi-Fi. The integration of sensors, actuators, and supporting hardware is presented alongside the system's power design. The control strategy and software implementation are then detailed, including the use of flowcharts and state diagrams to represent system behaviour. Finally, methods for data logging and remote monitoring are discussed, along with key limitations and considerations for future development.

5.5.1 System Requirements

The purpose of the microcontroller is to ensure that the machine functions as intended. This includes controlling misting and pumps, sensor monitoring, timing control, and safety handling. The microcontroller allows the automation of watering and environment monitoring. A set of requirements were listed within a

PDS. The following table shows the requirements that are more specific to the microcontroller and its system.

Table 10 - Key microcontroller related requirements

Requirement	Description	Target/Limit
Remote Access	The user should have remote access to the machine.	Access to sensor readings and machine state remotely
Humidity Deviations	The system shall respond to deviations in humidity within a specific time frame.	6 minutes
Misting Timing	The system shall control misting duration and interval with a resolution of 2 seconds.	2 seconds
Safety Shutdown	The system shall disable pumps and misting when water level falls below a defined threshold.	20% water level
Actuator control	The system shall control multiple actuators independently	N/a
Autonomy	The system shall operate without continuous user input.	User input should only be required once every 2 weeks
Offline Core Functionality	Core control functionality shall remain operational without Wi-Fi connectivity.	N/a
Data Logging	The system shall log data at defined time intervals.	Every 2 seconds
Sensor Readings	Read sensors at defined time intervals.	Every second

5.5.2 System Architecture

To meet the requirements listed in table 3 and other requirements in the PDS, several other components were required. These components allow functionality of the system as well as ensuring safe integration. Figure 11 shows a system architecture diagram splitting different components into a number of layers and showing communication/connection between these components.

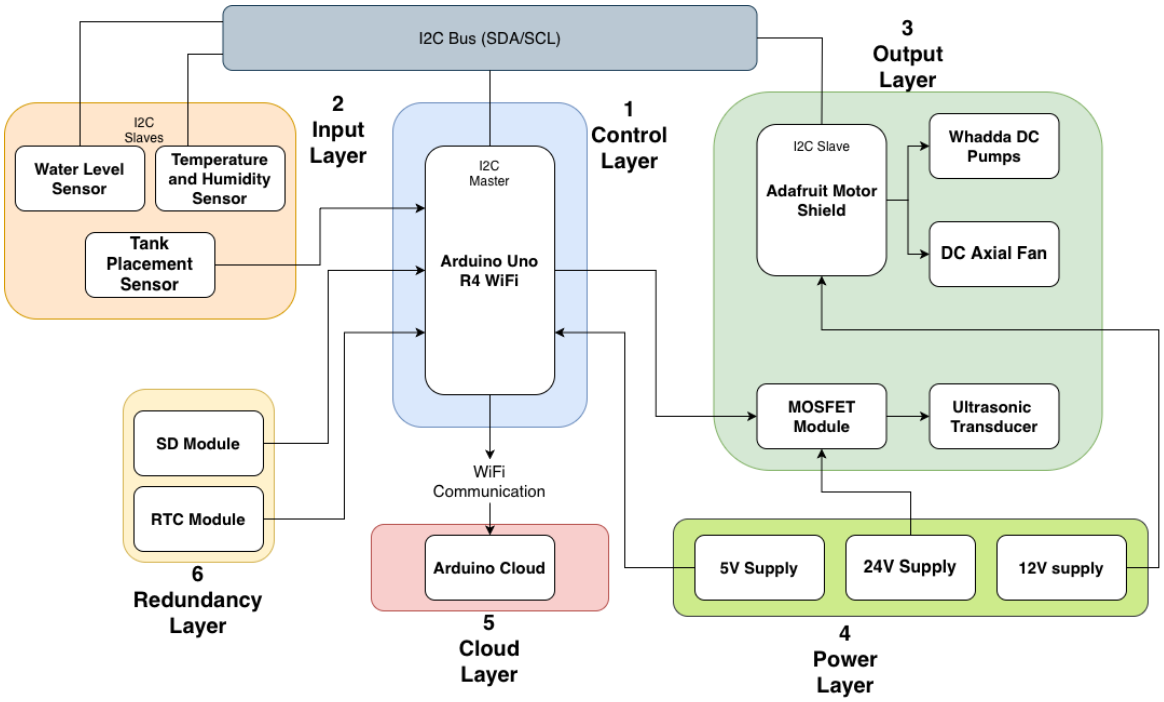

Figure 25 - System Architecture Diagram

To meet the requirements outlined in Table 3 and the wider Product Design Specification (PDS), the system was developed using a layered architecture, as shown in *Figure 25*. This approach separates sensing, processing, and actuation functions, improving system clarity, modularity, and ease of integration.

The control layer (1) consists of the Arduino Uno R4 WiFi, which acts as the central processing unit of the system. Layer 1 is responsible for coordinating all other subsystems by receiving sensor data, executing control logic, and issuing commands to actuators. A centralised control approach was selected to simplify system design and ensure consistent decision-making across all subsystems. The microcontroller

communicates with the input layer and the Adafruit Motor Shield via an I2C communication bus. In this configuration, the microcontroller operates as the I2C master, initiating communication with connected slave devices such as sensors and actuator drivers. The use of I2C reduces the number of required connections, enabling multiple devices to share the same communication lines and supporting future system expansion.

The input layer (2) consists of environmental and system-state sensors, which provide real-time data on conditions within the growing chamber. This information is used by the layer 1 to determine appropriate system responses. The output layer (3) includes actuators such as pumps, fans, and the ultrasonic transducer. These components are controlled either via the motor shield or through dedicated driver circuitry (e.g. MOSFET modules), as the microcontroller cannot directly supply the required current. These components are implemented to perform the functions required to maintain a suitable growth environment for the plants. In addition to the core control structure, supporting subsystems such as power distribution (layer 4) and communication modules are integrated to ensure reliable operation. The architecture is designed to be modular, allowing components such as sensors or mist generation methods to be modified without requiring significant redesign of the overall system.

The cloud and redundancy layers (layers 5 and 6 respectively) shown in *Figure 25* are dedicated to data logging and monitoring. These functions enable access to historical system data, supporting fault detection, performance evaluation, and analysis of environmental conditions for research purposes. The primary method of data logging is implemented through the Arduino Cloud, allowing users to remotely access system data via external devices. This improves usability and enables real-time monitoring during operation. A secondary, local logging layer is included in the system architecture as a redundancy measure. This ensures that data can still be recorded in the event of a loss of network connectivity, improving overall system reliability and robustness.

5.5.3 Microcontroller Selection

The selection of the microcontroller was a critical step in the system design, as it directly influences system capability, integration, and expandability. To meet the requirements outlined in *Table 10*, the microcontroller was required to support wireless communication, multiple sensor interfaces, and reliable actuator control. To enable remote access and IoT functionality, the microcontroller required integrated Wi-Fi capability. Additionally, compatibility with Arduino Cloud was necessary, as this platform was selected to provide remote monitoring and user interaction due to its relative simplicity, allowing more time to be allocated to prototyping, testing and other project tasks. Based on these requirements, the selection was narrowed to Arduino-compatible boards with integrated Wi-Fi. *Table 11* compares the two candidates.

Table 11 - Comparison of Arduino Uno R4 Wifi and Arduino Nano ESP32

Feature	Arduino Uno R4 WiFi	Arduino Nano ESP32
Arduino Cloud compatibility	Yes	Yes
Wireless communication	Yes	Yes
5V or 3.3V logic/sensor compatibility	Mainly 5V but able to connect to 3.3V sensors	Only 3.3V
I2C communication	Yes	Yes
Compatibility with Adafruit Motor Shield	Yes	No

Both candidates on top of Arduino cloud compatibility and Wi-Fi connectivity are also capable of a number of communication protocols such as I2C, which enables scalable integration of sensors and peripherals. Ultimately the Arduino Uno R4 WiFi was selected due to its direct compatibility with the Adafruit Motor Shield, which simplifies actuator integration and reduces the need for custom driver circuitry. This supports a more modular and reliable hardware design. The ability of the Arduino Uno to connect to both 5V and

3.3V sensors (although extra precaution needs to be taken with 3.3V sensors) also allows a wider range of sensor connections. Furthermore, the availability of the board within the laboratory environment enabled rapid prototyping and reduced development time, allowing greater focus on system integration and testing. While the Arduino Nano ESP32 offers a more compact form and greater processing capability, these advantages were not critical for this application. Therefore, the Uno R4 WiFi was considered the most suitable choice based on integration simplicity, functionality, and practical development constraints.

5.5.4 Hardware and Power Integration

This section describes the hardware interfaces used to connect the microcontroller to system components. These interfaces enable communication with sensors, control of actuators, and integration of supporting modules, ensuring that the system architecture can be implemented in practice.

Sensor Interfaces - Sensors are interfaced with a combination of I2C and GPIO connections, depending on device communication requirements. The use of GPIO connections has the benefits of straightforward integration into the system and remove the necessity for additional code required by I2C connections. This once again can improve the speed of prototyping and development, however, can reduce the flexibility in further sensor selection due to limited GPIO pins.

- Motor Shield – The purpose of the motor shield is to drive the pumps. The motor shield is controlled via I2C once again allowing multiple devices to share a common communication bus. It handles motor driving internally and simplifies the connections to actuators, allowing for more rapid prototyping.
- MOSFET Module - The ultrasonic transducer is controlled using a MOSFET switching module. This is required as the transducer operates at higher currents than the microcontroller can supply directly. The MOSFET allows a low-power control signal from the microcontroller to safely switch a higher-power load, ensuring reliable and safe operation of the mist generation system.
- Power Supply – Several approaches were considered for supplying power to the system components, including the microcontroller, motor shield, and ultrasonic transducer. The transducer requires a dedicated supply appropriate to its operating voltage and is controlled via the MOSFET module.

  The motor shield operates from a 12V supply, which can be provided either through the DC barrel jack of the Arduino Uno R4 WiFi or via its screw terminals. Supplying power through the barrel jack allows both the microcontroller and motor shield to share a common 12V source, whereas using the screw terminals would require a separate supply for the microcontroller. Although separate power supplies can improve stability by reducing the impact of voltage drops caused by motor operation, this increases system complexity. Therefore, a single 12V supply was selected to simplify integration while maintaining acceptable performance for the prototype system. Although a single 12V supply would simplify system integration, separate power supplies is the recommended approach by Adafruit [45].

5.5.5 Control Strategy

The control strategy defines how the system responds to sensor inputs to maintain suitable environmental conditions for plant growth. A hybrid approach is implemented, combining timed control for baseline misting cycles with feedback control based on real-time sensor data. The microcontroller continuously monitors environmental conditions and system states, making decisions to activate or deactivate actuators such as the misting system, pumps, and fans. Safety mechanisms are also incorporated, ensuring that the system enters a safe state under fault conditions, such as low water levels. This approach enables reliable, autonomous operation while maintaining flexibility for adjustment and optimisation.

The system follows a continuous control loop, where information is obtained through the input layer, a decision is made based on this information and an action is completed according to the decision. Figure 26 shows this simplified high-level control loop.

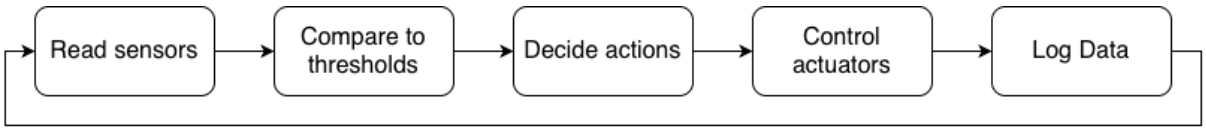

Figure 26 - Control Loop

- Environmental Control: The system regulates environmental conditions within the growth chamber based on sensor feedback. The primary parameter controlled is humidity, which is critical for effective nutrient uptake in an ultrasonic aeroponics system. The main way to control humidity for this system is through mist timings and intervals. When humidity falls below the threshold mist intervals are decreased to allow for more mist generation increasing moisture levels within the root chamber. Conversely, when humidity raises above the threshold it can be reduced by increasing mist intervals. However, careful consideration has to be taken when implementing nutrients into the system to ensure issues are not raised by reduced or increased nutrient levels. This feedback-based approach ensures that humidity is maintained within a suitable range for plant growth, while avoiding excessive saturation or drying of the roots.
- Timing Control: In addition to feedback-based control, the system incorporates timed operation to regulate misting cycles. This ensures that plants receive a consistent baseline level of hydration, even in the absence of significant environmental changes. Misting duration and intervals are controlled with a defined resolution, allowing adjustment of system behaviour based on experimental requirements. This hybrid approach improves system stability and prevents over-reliance on sensor feedback alone.
- Safety and Fault Handling: Safety mechanisms are integrated into the control strategy to prevent damage to components and ensure safe operation. Several features are included to reduce the risk of or prevent any hazards. One example is water level monitoring, where the system disables misting and pumping functions if the water level falls below a predefined threshold. This prevents the dry operation of pumps and transducers which could become damaged if this is not implemented. Other features also prevent actuator activity when the machine is not under safe operating conditions, such as the water tank not being inserted and sensor failures. The control logic described in this section is further detailed in the control flowchart (Section 5.5.7), which provides a step-by-step representation of system decision-making.

5.5.6 Control Flowchart

This section looks into a step-by-step flowchart showing how system control was implemented. *Figure 27* shows the flowchart which demonstrates the decisions that are made based on sensor readings and the resulting actions taken by the machine as a response to these sensor inputs.

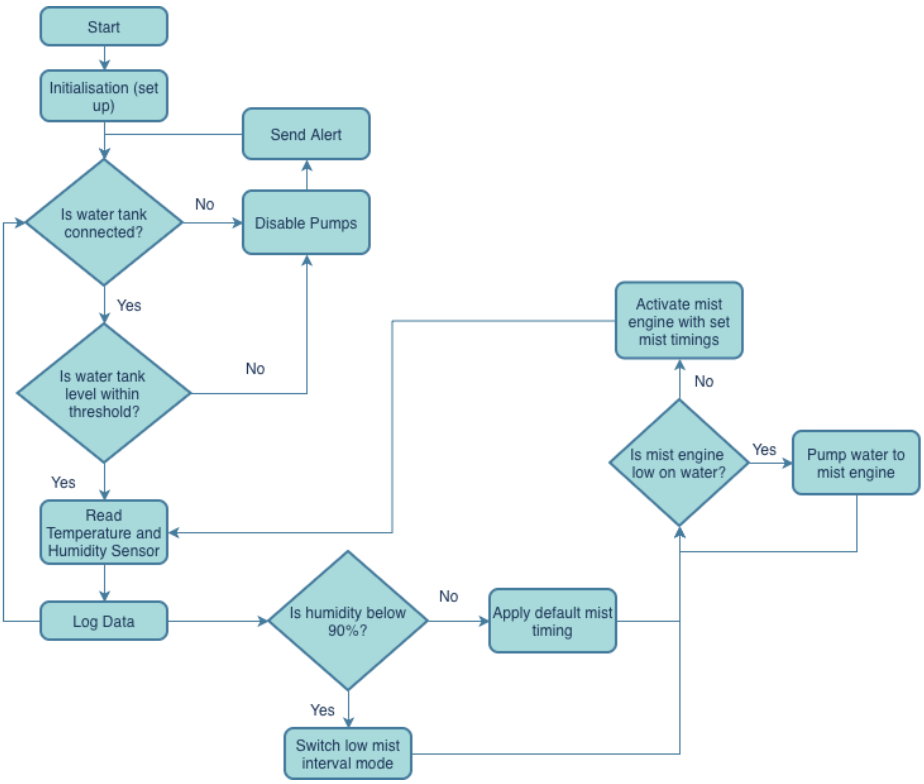

Figure 27 - System Control Flowchart

5.5.7 State Diagram

The state diagram illustrates the dedicated states of the system. Transitions into these states are governed by sensor inputs and control logic, allowing the system to respond dynamically to fault conditions. *Figure 28* shows the State Diagram. The different error codes shown in *figure 28* are defined here: W01 – Low Water (reservoir nearly empty), W02 – High Water (reservoir overfilled), L01 – Leak Detected (water in bund), F01 – Fan Failure, T01 – Chamber Overheat, A01 – Atomizer Overheat, I01 – Tank Missing, P01 – Primary Pump Failure (water not flowing to tray), P02 –Secondary Pump Failure (filtered water not flowing back into to tank), H01 – Low Humidity, H02 – High Humidity.

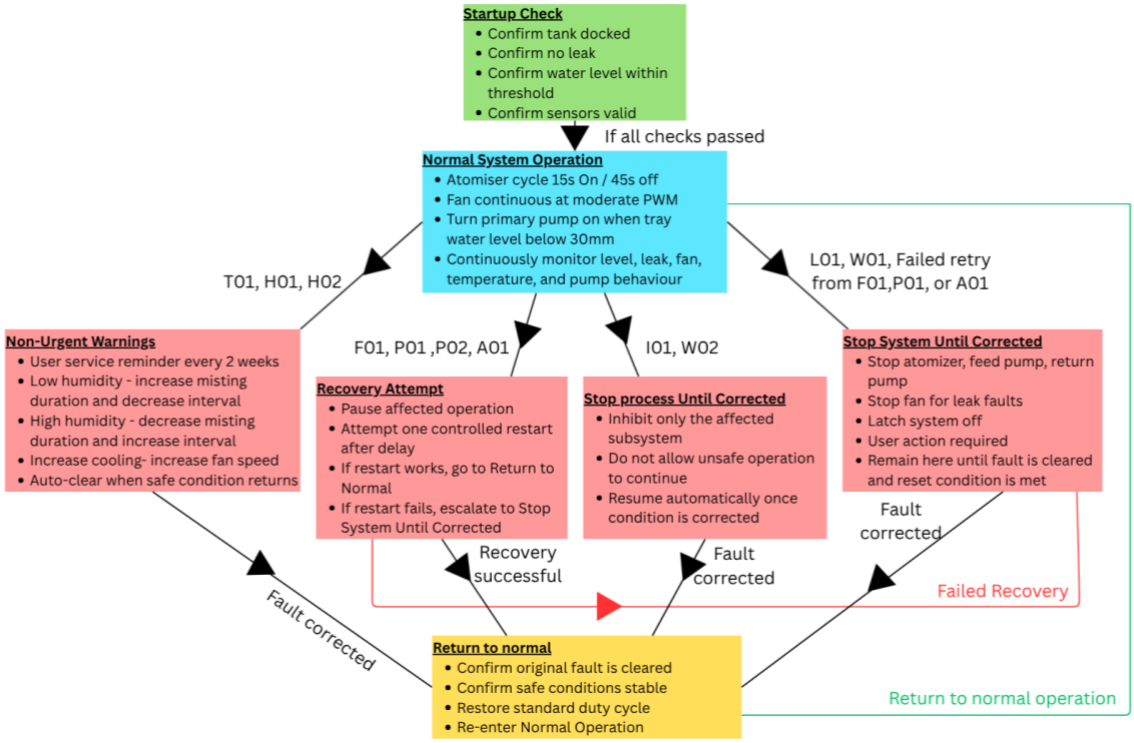

Figure 28 - State Diagram

5.5.8 Data Logging and IoT Integration

Data logging and remote monitoring are implemented using Arduino Cloud. This platform was selected due to its ability to provide rapid integration of IoT functionality with minimal development complexity, making it well suited to a prototype system. Arduino Cloud enables real-time monitoring of cloud variables through a dedicated user interface, which can be accessed remotely via external devices such as smartphones. These cloud variables can be assigned using Arduino Cloud and could be sensor readings or any other variables that would be useful for the user to know. Sensor readings are continuously updated and can be visualised using graphs, allowing trends in environmental conditions to be analysed over time. In addition, system states, such as actuator operation, can be monitored through cloud-linked variables. The platform also supports event-based notifications, where specific conditions (e.g. fault states or threshold breaches) trigger alerts to the user. This enhances system usability and allows prompt response to abnormal operating conditions during testing.

Alternative data logging methods, including the use of a real-time clock (RTC) and SD card module, were considered. These approaches enable local data storage and provide redundancy in the event of network failure. However, they were not implemented in the prototype due to the increased integration complexity. In a final design, a hybrid approach combining cloud-based and local data logging would improve system reliability.

5.5.9 Limitations and Design Considerations

A primary limitation of the system is its reliance on Arduino Cloud for data logging and monitoring. This introduces dependency on network connectivity, which can restrict testing environments and result in loss of functionality if a connection is unavailable. The absence of local data logging further reinforces this limitation.

The power system also presents a design trade-off. A single 12V supply is used to power both the microcontroller and actuator systems via the Arduino Uno R4 WiFi. While this simplifies integration, it may lead to voltage fluctuations due to varying load conditions from motors and pumps. Although acceptable for a prototype system, a more robust design would separate power supplies to improve stability.

Hardware scalability is also constrained by the use of general-purpose input/output (GPIO) connections for certain components. The limited number of available pins restricts the number of additional sensors or devices that can be integrated without redesign. While the use of I2C communication mitigates this to some extent, it is not applicable to all components.

Future improvements to the system would include the implementation of hybrid data logging using both cloud-based and local storage methods, improved power distribution design, and refinement of sensor selection to enhance accuracy and reliability.

5.6 Characterising environmental conditions of the growing environment (ST)

5.6.1 Introduction

The question this section aims to answer is, if the two 105kHz atomisers (selected at the time of simulation) and the design of the misting and root chambers can maintain the required environmental conditions. Computational Fluid Dynamics (CFD) was used to observe how the crucial physical quantities change over time and space of the root chamber. Specifically, temperature and water mass fraction (implying humidity) were monitored as they dictate the growing environment of the plant.

To do this, the cavity volumes of the root and misting chambers were prepared. Initial and boundary conditions on the domain (the cavity space where the mist disperses) were defined. A mesh sensitivity analysis was carried out to ensure that the resolution captured the plume dynamics with enough accuracy while maintaining computational feasibility. The simulation was then run over 180s with periodic misting, to see how the overall average of these quantities change. Simultaneously, the change in the quantities were also monitored each second over the whole domain.

5.6.2 Importance of Humidity and Temperature

Table 12 - Ideal Conditions

Physical quantity	**Importance**	**Ideal Conditions**
Temperature	Dictates the amount of oxygen in the water droplets, necessary for plant growth [46].	18-22°C [47].
Relative Humidity	Ensures the survival of the plant. Air is the only medium for water absorption and if not regulated correctly the roots dry out [48].	92% [49] equivalent to a mass fraction of 0.0133 based on *Equations 7 and 8* under Section 5.6.5

5.6.3 Geometry and Domain Preparation

To conduct the appropriate simulation, the relevant computational fluid domain was prepared. To do this the design of the misting and root chambers were used at the time of the simulation phase. Furthermore, the volume filled with water was removed, to only analyse the domain where the mist would disperse.

As illustrated in *Figure 29*, the domain was set up and imported in the CFD software Star-CCM+ with the appropriate regions labelled. The geometry shown was then partitioned so that the necessary boundary conditions were applied to the crucial surfaces (atomisers, outlets and the remaining walls).

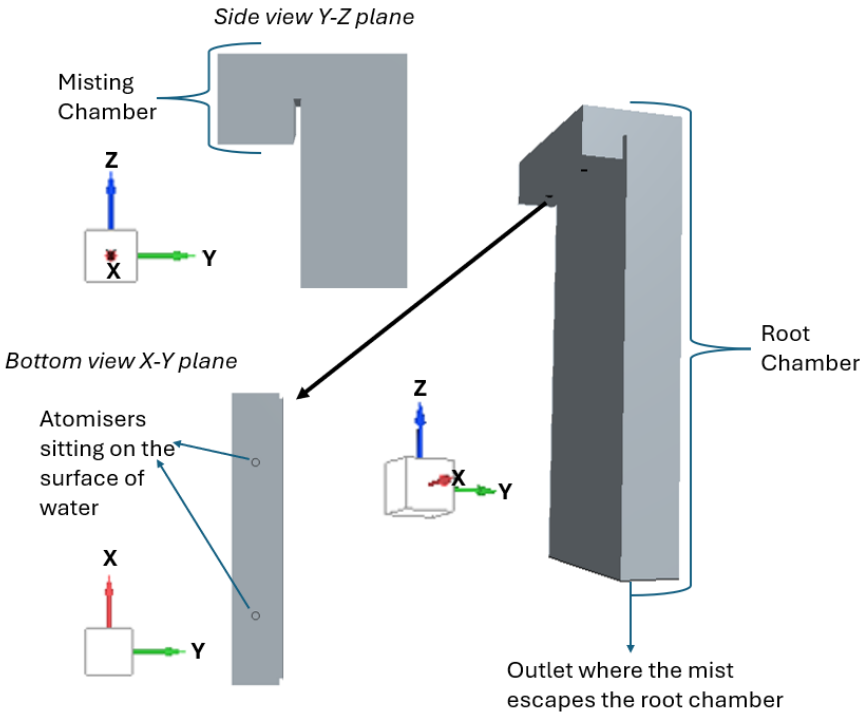

Figure 29 - The geometry of the domain with the main sections

5.6.4 Initial and Boundary Conditions

Atomisers

Table 13 - Atomiser Parameters

Input Parameters	**Value/Type**	**Justification**
Atomiser Diameter	8mm each	This is the diameter of the vibrating discs, which is the surface where the mist enters the domain. This was assumed based on the specs of the supplier [50]
Boundary condition	Wall with Lagrangian Injector	To accurately model the discrete water droplets entering the domain from the atomisers' discs, this boundary condition was assigned. The boundary regions represent the behaviour of air relative to them. Inlet wasn't assigned, as it would imply movement of air through that boundary which is false.
Atomisation duration	15s active and 45s rest	This was based on the 1:3 active-to-rest misting ratio utilised by an aeroponic report [51]. The cycle duration was scaled down to 60 seconds to make it computationally possible to simulate three full periodic cycles
Mass flow rate of mist	1.389×10^{-5} kg/s per atomiser	This is based off the assumption that 50mL/h of mist would be injected to the system for the specific atomiser [52].
Temperature of atomiser when active	311.15K (38 °C)	The atomisers vibrate at 105kHz and the long-term operating temperature is less than 40 ◦C [53]. Considering that it will vibrate for 15s and not all the Kinetic Energy will convert to heat due to the friction, the temperature is overestimated to be at 38 ◦C as a worst-case scenario. It was assumed that once at rest the atomizer returned to room temperature of 20 ◦C.

Outlet

The outlet's regional boundary was set as pressure outlet. It was set this way to allow the software to calculate how much air leaves the opening based on the pressure outside the domain. The gauge pressure

was set at 0Pa, considering that the outlet surface was assumed to be exposed to the atmospheric room pressure. This assumption was based on the outlet region not being airtight and preventing build-up of pressure.

Walls

The boundary region of the remaining surfaces was kept as wall. This is because there was no airflow through those surfaces. They were also assigned to be adiabatic as a worst-case scenario, to only observe the thermodynamic behaviour of the mist with no heat transfer to the surroundings.

5.6.5 General Physical Continua

To accurately capture the interactions of the mist and the air in the chambers, specific physical models were defined. The core models implemented were the following.

- Implicit Unsteady: This was set to analyse over real-time. Otherwise, the simulation would model until the point where equilibrium is reached without tracking the exact point in time.
- Multi-component Gas, Segregated Species and Segregated Fluid Temperature: These were set up to respectively model the property of humidity and temperature variations.
- Ideal gas model: To establish the thermodynamic relationship between pressure, volume and temperature within the fluid domain
- Lagrangian Multiphase: Provides the most representative way of simulating the mist. It treats the injected mist in terms of discrete water droplets rather than a continuous fluid.
- Multiphase Interaction: Enabled two-way coupling which allows the air to move the droplets and the droplets to cool the air.
- Gravity: Important for the current system, as the movement of the mist down the root chamber is relied on gravity, accounting the weight of the droplets.
- SST K-Omega turbulence model: To simulate the mixing of the mist with the ambient air and the boundary layer effects near the walls.
- Segregated Flow: This managed the relationship between pressure and velocity throughout the chamber.
- The initial relative humidity: Assumed to be 50% [54], based on the recommended humidity for UK homes. By using this humidity *Equations 7 and 8* [55] were used to find the mass fraction of water to be approximately 0.007 at 20 ◦C

$$P_{sat} = 610.78 \cdot exp\left(\frac{17.27 \cdot T}{T+237.3}\right), P_w = RH \cdot P_{sat} \quad (7)$$

$$\omega = 0.62198 \cdot \left(\frac{P_w}{P_{atm} - P_w}\right), Z = \frac{\omega}{\omega+1} \quad (8)$$

"T" is the temperature in ◦C, "P_{sat}" is the saturation vapour pressure in Pa, which is the pressure at 100% relative humidity. "RH" is the relative humidity (relative to the maximum amount of water vapour air can hold). "P_w" is the partial vapor pressure, which is pressure only caused by the water vapour at the relative humidity in Pa. "P_{atm}" is the atmospheric pressure assumed to be 101000Pa, "ω" is the specific humidity which shows the mass of water per unit mass of dry air, hence is unitless. "Z" is the mass fraction of water.

5.6.6 Specific Mist Properties

To resolve the physical behaviour of individual water droplets of the mist, the following properties and models were applied.

- Temperature: This was used to enable the heat transfer calculation between droplets and air.
- Quasi-Steady Evaporation: To simulate the rate at which the droplets transition to water vapor based on the temperature and pressure
- Initial temperature: They were set to have an initial temperature of 293.15K (20°C). This assumption is based on the bulk water reservoir temperature as well as the low power rating of 2W

of the atomisers which cause the atomiser's self-temperature to have a negligible effect on the thermal mass of the fluid.

- Drag Force and Pressure gradient: To simulate the kinematic and aerodynamic models of the water droplets
- Spherical Particles: To simulate the water droplets accurately. Their diameter was assumed to be approximately 20-micrometre as detailed in Section 5.3.4.

5.6.7 Mesh Sensitivity Analysis

The analysis was conducted to find a mesh size which compromises the computational power of the simulation and is reasonably close to convergence. Considering that the mesh analysis is used to find the acceptable resolution needed to capture the aerodynamics of the system, to isolate the spatial error from transient thermodynamic and humidity instabilities, the analysis was conducted under simplified steady-state and one way coupled conditions.

Furthermore, as shown on *Figure 30,* to capture the bends and the atomiser sections more precisely, a finer mesh was used. This was done because at the atomisers' faces, the mist is being injected in the domain at a significantly smaller surface area than the rest of the boundaries. Considering the bend is 180◦, there is a sudden change in the direction of the flow of the fluid which needs to be accurately captured. Hence to achieve this, a 7% of mesh base size was used for the atomiser mesh size and 25% of mesh base size was used for the bend mesh size.

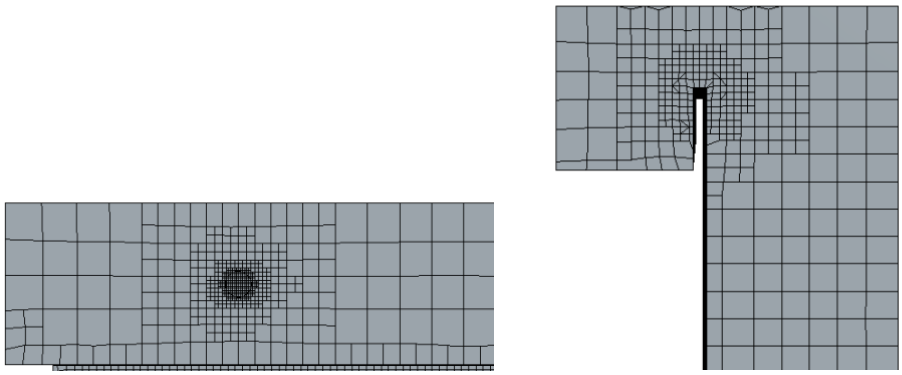

Figure 30 - The finer mesh shown at the atomiser face and at the bend

As shown in *Figure 30*, a hexahedral mesh was used. This mesh type was chosen because its cells align better with the vertical walls of the rectangular column. This allows the flow to be clear and perpendicular to the cell faces, minimizing numerical diffusion [56] and maintain computational efficiency.

Finally, as shown on *Figure 31,* different number of cells were investigated to monitor the effect on the outlet average velocity. It can be concluded that 138,000 cells (corresponding to 0.01m mesh base size) provide a sufficient balance between convergence and computational economy. The value of average outlet velocity of 0.001075 m/s is physically plausible. This is because considering the injected volume flow rate (Q_{in}), outlet area (A_{out}) in *Equation 3;* the actual outlet velocity (v_{out}) is found to be 0.00152 m s^{-1}. Therefore, the percentage difference from the real value is around 30%. This level of difference is acceptable considering that there are dead zones in the corners of the rectangular outlet hence less of the outlet area is used. Therefore, even though higher local velocity in the centre would result, the overall average velocity is lower than expected.

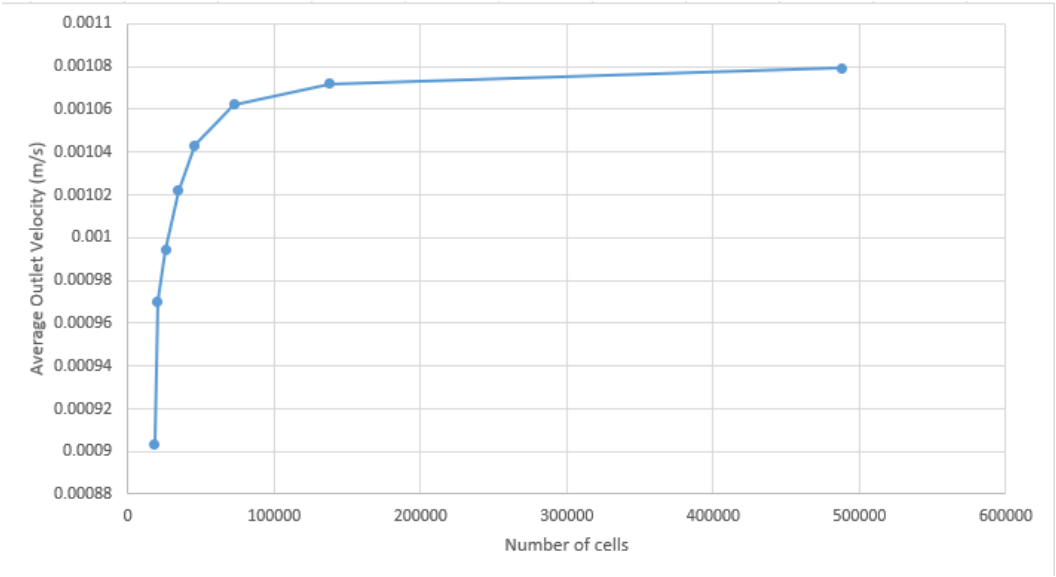

Figure 31 - Graph showing convergence after 0.01m mesh base size

$$Q_{in} = v_{out} \times A_{out} \quad (3)$$

5.6.8 Results

The original physical parameters were then set, to simulate the mist flow in 3 cycles of 15s active atomisation and 45s rest. Considering that the domain was symmetrical; to optimize computational efficiency, a symmetry plane was applied to cut the fluid domain in half. In the simulation the temperature and mass fraction of water were monitored.

<u>First Cycle (0-60s)</u>

As shown on *Figure 32,* for the first 15s, the mist was being injected to the domain, where evaporative cooling caused the average domain temperature to drop to 280K (7◦C). Simultaneously, the mass fraction of water increased to 0.018 as more mist was being added to the system. This mass fraction of water represents a relative humidity of 100% with a dense mixture of both air and mist.

For the next 45s, the temperature rose to 311K (38◦C) as evaporative cooling stopped. The mass fraction also decreased to 0.014 as the mist left the domain.

<u>Divergence</u>

While the initial cycle gave a physically plausible trend, the remaining cycles experienced a clear numerical divergence, as the average temperature escalated to 380K (107◦C). Given that the maximum thermal input of the atomisers was at 311.15K, reaching 380K violates the First law of Thermodynamics. This implies that the CFD solver was artificially generating thermal energy within the domain, as there is no powerful heat source present which can add enough thermal energy to reach 380K.

The divergence had been caused by a combination of limitations in frames per second, numerical instability and physical boundary constraints.

- Time-Step Resolution: To simulate 180s of real-time simulation over 3 hours, a relatively large time-step was implemented. The time step wasn't small enough to capture the shift from the atomizer turning from on to off and vice versa, which caused a severe computational shock. This shock caused errors in the solver's equations leading to temperature overshoots.
- Poor Condensation Modelling: The model did not account for vapor condensation on the colder walls. Realistically, warm liquid droplets would appear on the ceiling and walls. They would fall by gravity, carrying thermal energy downwards preventing heat build-up at the top of the root chamber.

- Adiabatic Constraints: The simulation used adiabatic walls as an overestimation. This was to observe the thermal behaviour of the mist in the domain, without heat transfer with the walls. However, realistically there would be constant heat transfer through the walls due to the thermal gradient.

5.6.9 Design Considerations

The fundamental spatial fluid dynamics shown on *Figure 33* can be used to consider design improvements, after confirming this effect with physical tests.

As shown on *Figure 33* when the atomiser is in rest mode, the push of mist by the atomisers is stopped, and the system is driven by natural convection. Heavier and colder droplets are pulled down to the outlet by gravity, while warmer water vapor rises to the ceiling of the root chamber. Even though the temperature divergence exaggerated the effect of natural convection, the process itself could still physically occur. If it isn't addressed properly, the upper sections of the root chamber would suffer from oversaturation of vapor, and the lower section would have roots dried out.

To prevent this from happening, an airflow must be introduced in the system from the root zone ceiling downwards. Incorporating a fan at the top of the root chamber could overcome the natural buoyancy of warm vapor. The forced convection from the fan would ensure that moisture evenly distributes throughout the root chamber and prevents areas of the domain with higher temperatures.

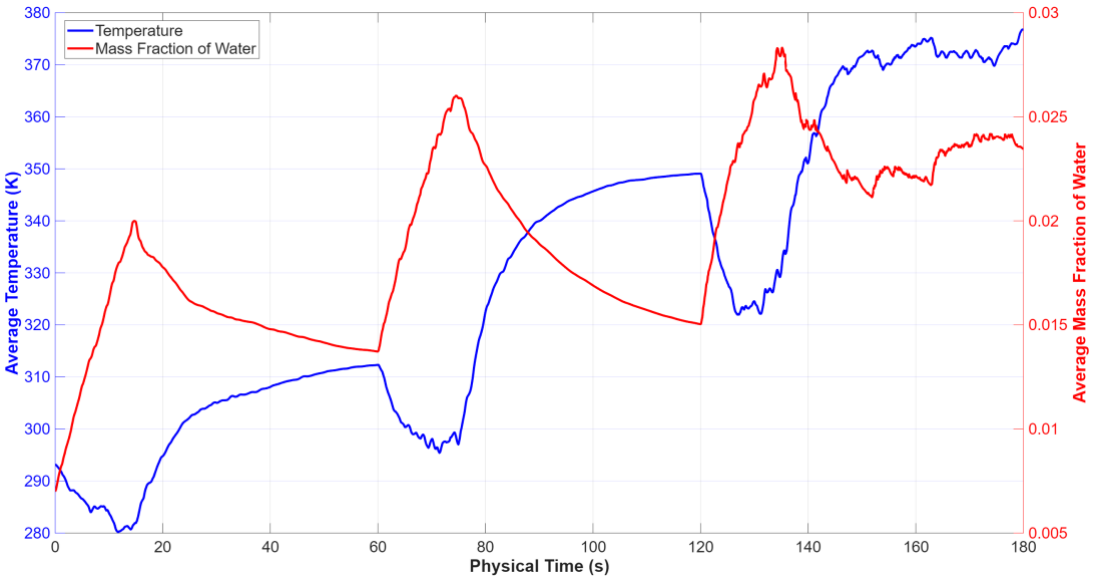

Figure 32 - Average Temperature and Mass fraction of Water over time graphs

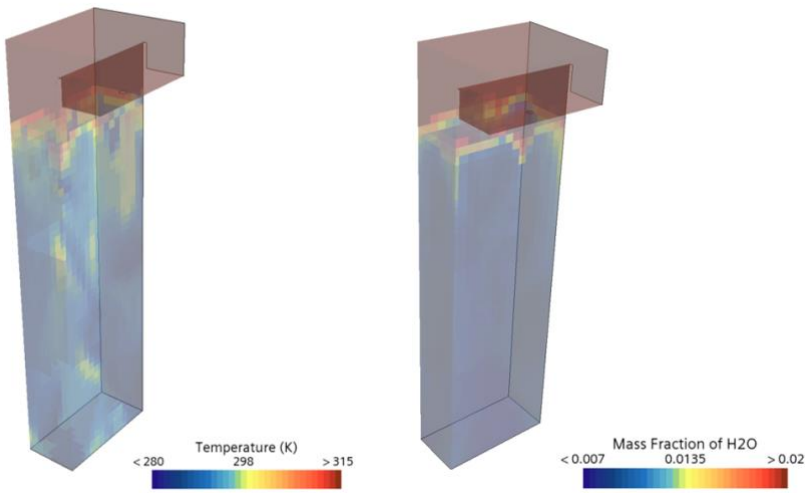

Figure 33 - Colour Maps of Temperature and Mass Fraction of Water over half of the volume of the chambers at the 100th second when misting is tuned off

5.6.10 Relevance to New Design

Although the final assembly used a modified chamber geometry and a commercial mist maker, the core aerodynamic results of this simulation remain relevant. The mist maker operates in an identical principle to the atomizers, where mist is generated with similar thermodynamic properties. Furthermore, the final design operates with the similar sealed column. It relies on misting occurring at the top, and the mist moving by gravity down the root chamber. Therefore, the system still has the risk of natural convection from occurring. However, this was further tested in real practice to verify the effect.

6 Detailed Design (EG)

6.1 Approach

The detailed design phase produced final part geometry, tolerance and fastener schedules, the complete bill of materials and a step-by-step assembly procedure. Owing to the page allocation of this report and the project's open-source intent, this material has been published in full as an Autodesk Instructables build log. This section therefore summarises the manufacturing scale, presents the assembled prototype and indexes the externally hosted documentation.

6.2 Manufacturing Summary

Fabrication followed the strategy outlined in Section 5.2.5. The completed prototype comprised 101 unique 3D-printed components, supported by a 20mm aluminium T-slot frame, fasteners, gaskets and the auxiliary components catalogued in Section 5.4. Aggregate filament consumption and print time are summarised in *Table 14.*

Table 14 – Aggregate Filament Consumption

Filament	Mass (g)	Print time (hrs)	Primary Application
PETG HF	5,364	133.35	Wet zone components, structural enclosures, lids
PETG Translucent	1,106	45.02	Sanitisation Tank, Filtration Region
Wood PLA	2,036	52.53	External façade panels
TOTAL	**8,509**	**230.9**	

All parts were printed on a Bambu Lab P1s with a 0.4mm hardened steel nozzle and 0.2mm layer height. Per-component wall counts and infill densities followed the rationale described in Section 5.2.5.

6.3 Build Prototype

The fully assembled prototype is shown in Figures X-Y. External dimensions of 853mm tall with a 183x358mm base footprint were achieved. All components specified for incorporation throughout Section 5 were physically integrated, apart from the Tank Latch Mechanism *(8).*

Permanent assemblies in the Mist Chamber *(2)* and Filtration Region *(11)* were bonded with clear two-part epoxy at the tongue and groove joints validated in Section 5.2.5. Serviceable assemblies used heat-set brass inserts with countersunk screws. Wet-region seals were achieved using O-rings and gaskets lasered from a silicone sheet, in accordance with Section 5.2.4.

Figure 34 – QR Code to Instructables Page

6.4 Open-Source Publication

The Instructables build log contains the material omitted from this report:

- Full BoM with supplier part numbers & unit costs
- STEP files for every printed component, with print orientation and slicer profile guidance
- Step-by-step photographic assembly procedure
- Microcontroller wiring diagram and pinout reference
- First-boot, sensor calibration and Arduino Cloud setup instructions

All design files are released under CC0 1.0 (public domain dedication), satisfying the project's open-source aim and enabling independent reproduction or extension by the wider community. A QR code to the page is presented in *Figure 34*.

7 Testing

7.1 Test Plan (EC)

The purpose of this test plan is to verify the functionality, performance, and safety of the aeroponic system. As well as to optimise processes to improve the machine's performance. Testing focuses on validating control behaviour, system responsiveness, and safe operation under both normal and fault conditions.

7.1.1 Test Plan Table

Table 15 - Test Plan

ID	Test Name	Method	Metric	Target
F-01	Actuator Functionality	Test run actuators using the microcontroller.	Functional (binary)	Actuators visibly turn on and function.
F-02	Binary Sensor Accuracy Test	Read binary value sensors during known conditions.	HIGH/LOW	Readings are expected based on conditions.
F-03	Mist Timings Test	Record timings of mist maker being on or off.	Time (s)	90 s ON, 360 s OFF
F-04	Measurement accuracy	Record temperature, humidity and distance under known conditions	Error (°C, %, mm)	± 1.0 °C ± 1% ± 4 mm
F-05	System Control Logic Response	Simulate environmental changes (e.g. humidity drop). Record time to bring back to normal conditions.	Response time (min)	6 minutes to return to above 90%
I-01	Arduino Cloud Variables	Observe cloud dashboard for sensor readings.	N/a	Cloud variables are displayed on dashboard in Arduino cloud.
I-02	Tank water level low trigger	Drain tank and observe alert detection.	Water Level (%)	<10%
P-01	Mist distribution test	Observe mist flowing into root chamber.	Mist distribution	Mist should be distributed evenly.
S-01	Tank placement test	Disconnect tank during operation.	Response time (s)	Pumps are off within 2 s
S-02	Tank Level Low test	Gradually drain tank to below 10%	Response time (s)	Pumps are off within 2 s
S-03	Mist Engine Water low	Slowly drain water level and observe actuators	Response time (s)	Mist maker is switched off and water pumped to misting tray within 2 s
T-01	Mist Timings Optimisation	Test several mist timings and record temperature and humidity.	Temperature (°C) and RH (%) deviation	Mist timings with least deviation from 23 °C and above 90 % RH.

7.1.2 Mist Timings Optimisation

Test T-01 was conducted to determine ideal misting intervals and durations for maintaining stable environmental conditions within the root chamber. A range of mist intervals and durations were tested to

determine the ideal timings. Misting durations ranged between 90 to 120 seconds, whilst misting intervals were tested between 300 to 420 seconds (these ranges were obtained from [57]).

A set of misting intervals and durations were tested for several cycles to determine their effects over reasonable amount of time. For each set temperature and humidity data was recorded over time using the systems sensors with results monitored through Arduino Cloud.

The performance of each configuration was evaluated based on the system's ability to maintain humidity within the desired range, while avoiding rapid oscillations or excessive saturation. Through this process a set of optimised misting parameters were identified and implemented within the control strategy.

7.2 Test Set-up (EC)

7.2.1 Machine Set Up

The system was tested as a fully assembled unit under normal operating conditions, as shown in *Figures 34 and 35*.

Figure 34 - Back of the machine showing the root chamber, with the misting chamber on top and pump compartment at the bottom.

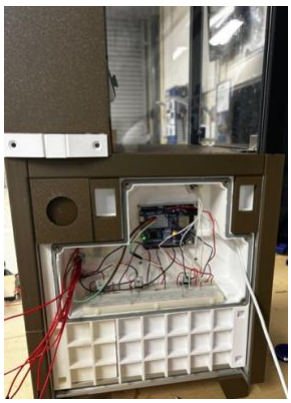

Figure 35 - Machine's electronics case showing the microcontroller and supporting circuitry.

7.2.2 Data Collection

Sensor data was monitored via the microcontroller and recorded through both Arduino Cloud and the serial monitor during operation. For tests requiring timing measurement both the serial monitor and a stopwatch were used. *Figure 36* shows the Arduino Cloud dashboard collecting data on humidity and temperature as well as showing things like whether the tank is connected.

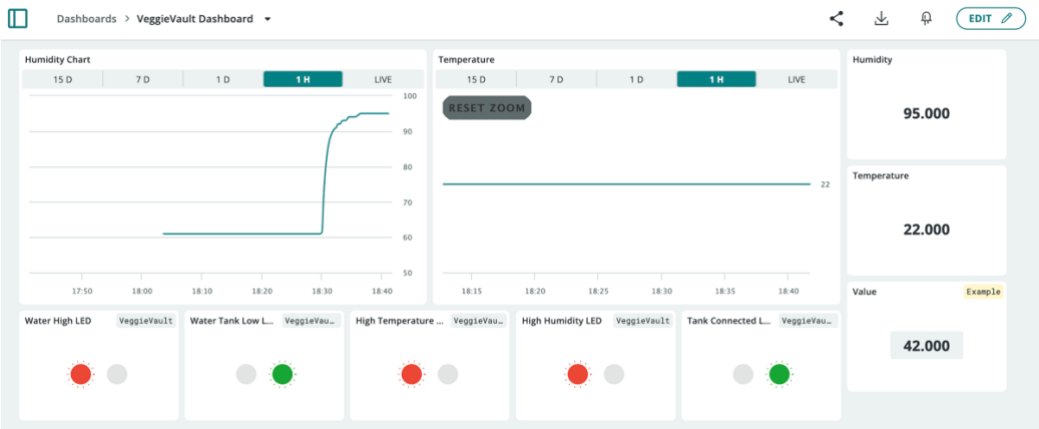

Figure 36 - Arduino Cloud Dashboard

7.2.3 Measurement Limitations and Implementation Issues

Due to practical constraints during assembly, the intended high-accuracy temperature and humidity sensor could not be implemented. A substitute sensor (DHT11) was used which provided approximate

environmental readings under normal room conditions. However, this sensor exhibited limitations in high-humidity environments. It was unable to measure relative humidity above 95% resulting in saturation. As a result, humidity measurements in the roots chamber are considered indicative rather than fully quantitative.

Further issues were discovered with one of the VL53L1X distance sensor, where due to the longer wires required by its placement an I2C connection was unable to be made meaning water level measurements in the misting tray were unable to be made. As a result, water level control was implemented using timed pump activation based on the water usage of the mist maker.

One further set up modification was made after initial tests involving the Adafruit Motor Shield. Brushless pumps were driven using MOSFET switching rather than the motor shield. This was due to compatibility issues between the pumps and the motor shield.

7.2.4 Test Conditions

Testing was conducted at room temperature (roughly 22 °C) using tap water. Depending on the test being conducted the system either just operated on a start-up or operated continuously for a period of time required by the test.

7.3 Results and Evaluation (EC)

The test plan was carried out with the test set up described above. *Table 16* shows the results of the tests; the requirement associated with the test and whether the requirement was met.

Table 16 - Testing Results

ID	Requirement	Target	Result	Status	Notes
F-01	Actuator functionality	Operates when triggered	Pumps and mist maker operate via MOSFET	Pass	Motor driver unable to drive pumps. MOSFET used.
F-03	Mist timing control	90 s ON / 360 s OFF	Achieved within ± 2 s	Pass	Meets control requirement
F-04	Measurement accuracy	± 1 °C / ± 2% RH	± 2 °C / ± 5% RH	Failed	The DHT11 isn't as accurate as the chosen SHT85
F-05	Control Response	<6-minute recovery	<2-minute recovery to above 90% RH from 61%	Pass	Misting quickly drove to above 90% and remained above this threshold during normal operation.
I-02	Tank water level low trigger	Trigger sent at <10% tank water level	Detected and trigger sent	Pass	Notification sent when water tank reached below 10% water level
P-01	Mist distribution	Even distribution	Mist spread throughout the tank, unable to tell if there were concentrations	Pass	Tentative pass as unable to accurately determine distribution of mist. Visually even.
S-01	Tank connection	Pumps stop within 2 seconds of tank being disconnected.	Pumps stopped operation after 1.5 seconds once tank was disconnected.	Pass	Tank disconnection was detected quickly, but switching pump off took longer.
S-02	Tank Level Low	Pumps stop within 2 seconds when water below 10%	Pumps stopped operation after 1.5 seconds once tank was disconnected.	Pass	Water level detected quickly but switching pump off took longer
S-03	Mist Engine Water Low	Mist maker switched off when water is low and water is pumped to misting tray.	Unable to detect water level in the misting tray. But mist maker used its own sensor to prevent dry operation.	Fail	I2C sensor communication was not established due to long wires so water level control was switched to timings.
T-01	Environmental stability	As low a deviation as possible from 23 °C and above 90% RH	Temperature achieved. RH raised above 95%	N/a	Unable to accurately measure humidity, but temperature didn't deviate no matter the timings.

7.3.1 Key Findings

Overall, the system was able to carry out the majority of its functionality. Safety features were all confirmed to be working as intended with actuator shutdowns under the correct conditions being performed within the required response times. The system was able to carry out its primary function of generating and maintaining a high humidity environment as well as perform further functions that aided the primary one. However, issues with sensors resulted in control logic needing to be modified and the inability to effectively carry out some tests. Issues with compatibility of the motor shield and pump, as explained in the test set up, had little to no effect on results.

Several issues were identified during testing which had a significant effect on results. The first was the inability to use the VL53L1X distance sensor in the mist chamber. The length of the wires resulted in the sensor unable to establish an I2C connection with the microcontroller meaning it was unusable. This caused the control logic to change to a timing-based logic (which was calculated to be 8.2 seconds on and 58 minutes off). This meant test S-03 was not able to be carried out as intended, although the mist maker had its own sensor meaning it would switch off if water levels were too low.

Another significant issue was the use of the DHT11 rather than the SHT85 temperature and humidity sensor. The SHT85 was unable to be implemented due to issues with preparation for integration. The DHT11 encountered issues with saturation at 95% RH. The sensor was simply unable to measure above this value, which although would still be in the preferred range of 90% to 100% RH [58], meaning humidity behaviour was unable to be determined. The DHT11 was also subject to measurement inaccuracies caused by moisture inside the sensing element, meaning humidity remained at 95% (when it likely wasn't) even when the mist maker was switched off for a prolonged period of time. This caused issues in obtaining accurate results for tests such as F-05 and particularly T-01.

7.3.2 Design Implications

These findings indicate that design modifications should be made for future iterations. Particularly fixes to sensing methods as these had significant effects on testing. Improvements to the control strategy could likely be made as well, however testing has kept it unclear whether significant control changes need to be made.

With regards to the distance sensor in the mist chamber, several options exist to fix the issue. A different sensor that does not use an I2C communication protocol could be implemented making the need for longer wires not an issue. However, this could potentially cause further issues when increasing the number of sensors as there are limited GPIO pins. This would not be an issue with an I2C sensor. The VL53L1X distance sensor could still be implemented alongside an I2C range extender such as an active terminator to allow for longer wires. Wire modifications may have to be made to implement this solution.

Issues regarding the DHT11 would be fixed with the SHT85 which was initially chosen to measure temperature and humidity. It would increase accuracy (with $\pm$1.5% RH and $\pm$0.1 °C accuracy instead of $\pm$5.0% RH and $\pm$2.0 °C accuracy). Issues with saturation would also be fixed as the measurement range for the SHT85 is 0% to 100% RH. The SHT85 also contains measures to mitigate the effects of condensation reducing errors caused by this.

Further investigation should be made into ideal mist timings as this was unable to be done due to the limitations of the DHT11. A reasonable range has been determined through research, however experiments looking into the effect of mist timings on the stability of humidity and temperature should be conducted.

8 Future Work (ST)

As mentioned in the PDS section of the report, nutrient management, pH control and root oxygenation were outside the scope of the final design. The primary focus was on the development of the mechanical and electronic architecture for automation, alongside maintaining the right temperature and humidity for the plants' roots region. However, supplying the right amount of nutrients, maintaining the right pH, as well as allowing oxygen supply to the roots is essential for plant growth.

8.1 Nutrients and pH

8.1.1 Importance

Optimal plant yield especially in fogponics depends on maintaining nutrient concentration and pH levels. Both macro and micronutrients are crucial for plant growth [59], their supply in terms of concentration must be carefully regulated to prevent toxicity or nutrient deficiency [60]. Controlling the pH is also fundamental, because it dictates the availability of the nutrients to the plant roots [61].

8.1.2 Design Considerations

The proposed design of the water tank shown on *Figure 37*, highlights the integration of nutrient and pH to the main water tank of the Fogponic design. With the appropriate sensors and pumps, the system ensures optimum root conditions for plant growth.

- Nutrient Management: Using Electrical Conductivity (EC) sensor and a nutrient injector, the system will add nutrients when the EC detects a fall in concentration below 0.64 dS/m. This value is determined from the ASHS hydroponic study, where 1.6 dS/m gave moderate fresh weight of plants [62]. However, fogponics uses 60% less nutrients due to efficiency [63] hence 0.64 dS/m is used as the threshold
- pH Management: Via a pH sensor and secondary tanks containing the phosphoric acid and potassium carbonate (alkali) separately, to maintain the pH at 5.8 as mentioned in the ASHS study.
- Water Level: Using a water level sensor and a floater, atomised and sterilised water is added to the tank via a peristaltic pump after it has been used for misting.
- Water Supply to the misting chamber: By coordinating the water level sensor of the misting chamber and the main water pump, water is supplied to the chamber from the main water tank.

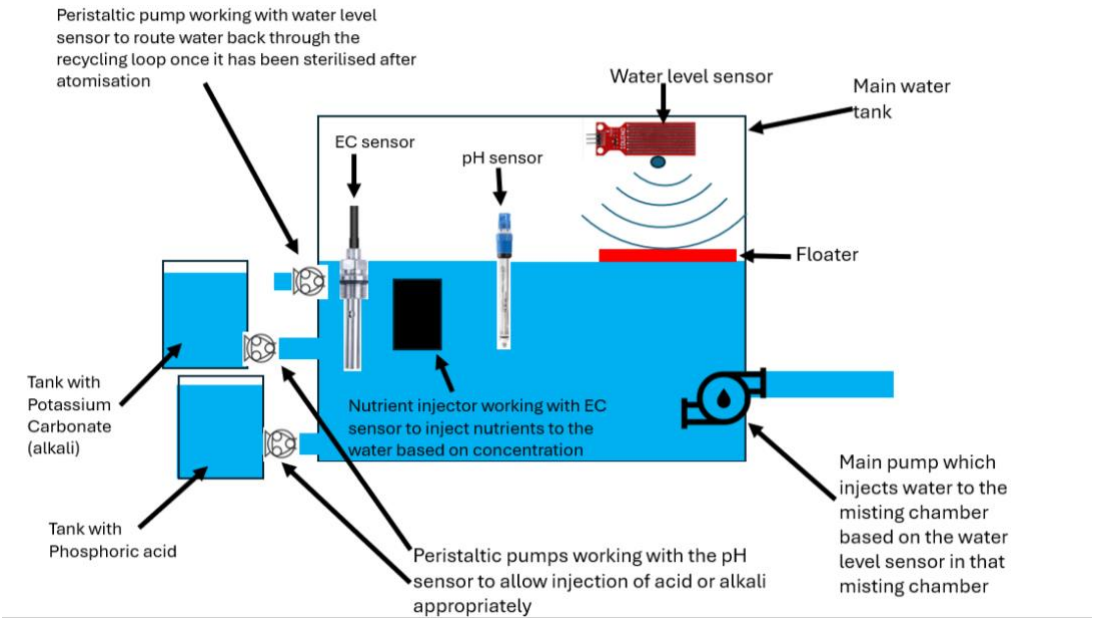

Figure 37 - Nutrient and pH design consideration

8.2 Oxygenation

8.2.1 Importance

The Fogponic system has a closed/isolated air flow, which is a system where outside air isn't added, or the inside air isn't removed. This means that, there will be an initial amount of oxygen in the system which will be depleted by the roots [64]. Therefor the challenge is that, due to constant oxygen absorption, its total amount is being decreased, leading to its deficiency to the roots for plant growth. Therefore, alternative methods must be considered to introduce oxygen into the system without actively interfering the movement and accumulation of the mist.

8.2.2 Design Considerations

Adding the oxygen content of the water reservoir before the atomization occurs, is one way to tackle the issue of oxygen deficiency. This can be done by incorporating air stones in the water tank [65]. They work with an air pump and airline (pipe carrying air). The outside air is compressed and pumped through the air line and pushed out of the air stone inside the water tank. The challenge is that, by pushing air inside the Fogponic system via the air stone will decrease the concentration of the mist which could reduce the supply of nutrients and oxygen to the root. A way to solve this is using two separate reservoirs. The main water tank can be used for the oxygenation of water allowing air to enter through the air stone and exit via an opening (to prevent build-up of pressure). Then this oxygenated water can be pumped to the reservoir where atomization will occur (misting chamber) with a fresh supply of oxygenated water.

An alternative way to promote oxygenation of water is by agitating the surface of the water tank to promote gas exchange [66]. This can be done by creating a waterfall like effect in the system where the recirculated water from the root chamber falls into the water tank. Also, air must be effectively circulated in and out of the water tank for constant supply of oxygen. This can be done by venting the water tank.

9 Conclusion (FM)

This project aimed to address the need for an automated, domestic crop-growing system by developing an open-source fogponics machine. Through a structured design process, the team successfully manufactured a 3D-printed prototype powered by a 1.7MHz ultrasonic atomizer and an Arduino microcontroller.

System testing verified that the core mechanical architecture and automated control logic function as intended. The prototype successfully generated a dense mist to maintain high humidity in the roots chamber and reacted correctly to safety faults, such as shutting down actuators when low-water level was detected. However, the testing phase also highlighted some hardware limitations. The substitute DHT11 sensor for temperature and humidity control in the roots chamber saturated at 95% relative humidity, and long wire lengths cause I2C communication failures with the misting tray's water level sensor.

Due to time constraints, this initial prototype focused entirely on mechanical and electrical validation using pure water. Testing the machine on plants, including the integration of nutrients, pH control, and LEDs grow lights, was excluded from the current scope.

Ultimately, the project successfully proved mechanical feasibility of a domestic fogponics unit. For the system to evolve into a fully viable commercial product, future developments must focus on three key areas: transitioning the structure from 3D printing to scalable manufacturing processes, integrating the automated nutrient and pH dosing systems, and upgrading the atomization module to ensure reliable performance when exposed to chemicals.

Bibliography

[1] A. Nursyahid, T. A. Setyawan, K. Sa'diyah, E. D. Wardihani, H. Helmy and A. Hasan, "Analysis of DWC hydroponic nutrient solution level control systems," 2021. [Online]. Available: https://iopscience.iop.org/article/10.1088/1757-899X/1108/1/012032/pdf.

[2] A. D. Jani, T. D. Meadows, M. A. Eckman and R. S. Ferrarezi, "Automated ebb-and-flow subirrigation conserves water and enhances citrus liner growth compared to capillary mat and overhead irrigation methods," 1 March 2021. [Online]. Available: https://www.sciencedirect.com/science/article/pii/S0378377420322551?casa_token=76ZTufZ-BcAAAAAA:HVjaSXuFXcJsiaZiCPBANsWOsnBvvdiN5TtId9Ze_tYOICVt8_gj-GgqbdmL5NEmGyh5jeMuOg.

[3] Plantechology, "6 Popular Hydroponic Systems Explained - Find Your Perfect Match," 12 August 2025. [Online]. Available: https://www.plantechology.com/en/blog/6-popular-hydroponic-systems-explained-find-your-perfect-match.

[4] C. McDonald, "Ebb and Flow vs DWC: Growing Systems Compared," 20 February 2023. [Online]. Available: https://www.plantechology.com/en/blog/6-popular-hydroponic-systems-explained-find-your-perfect-match.

[5] H. A. Abdulrazzaq, O. I. Jerca, V. Bobutac and E. M. Draghici, "Comparative study on lettuce growing in NFT and Ebb and flow system," [Online]. Available: https://www.horticulturejournal.usamv.ro/pdf/2021/issue_1/Art50.pdf.

[6] Simple Greens Hydroponics, “4 Reasons Why I Don't Use NFT for Hydroponics,” [Online]. Available: https://www.simplegreenshydroponics.com/blog/4-reasons-why-i-dont-use-nft#:~:text=As%20the%20plants%20grow%2C%20the,commonly%20grown%20in%20NFT%20systems.

[7] M. Samangooei, P. Sassi and A. Lack, “Soil-less systems vs. soil-based systems for cultivating edible plants on buildings in relation to the contribution towards sustainable cities,” 2016. [Online]. Available: https://thefutureoffoodjournal.com/manuscript/index.php/FOFJ/article/view/91.

[8] B. M. Eldrige, L. R. Manzoni and C. A. Graham, “Getting to the roots of aeroponic indoor farming,” 2020. [Online]. Available: https://nph.onlinelibrary.wiley.com/doi/epdf/10.1111/nph.16780.

[9] M. R. Uddin and M. F. Suliaman, “Energy efficient smart indoor fogponics farming system,” 2021. [Online]. Available: https://iopscience.iop.org/article/10.1088/1755-1315/673/1/012012/pdf.

[10] Nasa, “How to write a good requirement - Checklist,” 26 July 2023. [Online]. Available: https://www.nasa.gov/reference/appendix-c-how-to-write-a-good-requirement/.

[11] C. Mullins, A. Vallotton, J. Latimer, T. Sperry and H. L. Scoggins, “Hydroponic Production of Edible Crops: Deep Water Culture (DWC) Systems,” 19 July 2023. [Online]. Available: https://www.pubs.ext.vt.edu/SPES/spes-464/spes-464.html.

[12] H. A. A. Al-Kinani, O. I. Jerca, V. Bobuțac and E. M. Drăgichi, “COMPARATIVE STUDY ON LETTUCE GROWING IN NFT AND EBB AND FLOW SYSTEM,” *Scientific Papers. Series B, Horticulture.,* vol. 65, no. 1, pp. 361-368, 2021.

[13] J. R. Farmer, B. G. Crowther and C. D. Guy.Unite Kingdom Patent GB2567630A, 2019.

[14] Vext, “Vext 2.0 Smart Garden,” Vext, 2026. [Online]. Available: https://vext.fi/products/vext-2-0. [Accessed 2026].

[15] Q. Phan, A. DuBois, J. Osborne and E. Tomasino, “Effects of Yeast Product Addition and Fermentation Temperature on Lipid Composition, Taste and Mouthfeel Characteristics of Pinot Noir Wine,” *Horticulturae,* 2022.

[16] Vext, “Vext 2.0 Technical Specifications,” Vext, 2026. [Online]. Available: https://vext.frontkb.com/en/articles/4072642. [Accessed 2026].

[17] Vext, “FAQ,” Vext, 2026. [Online]. Available: https://vext.fi/pages/faq. [Accessed 2026].

[18] CPC, “PLCD16004 1/4 Hose Barb Valved Panel Mount Coupling Body,,” CPC, 2026. [Online]. Available: https://www.cpcworldwide.com/General-Purpose/Products/Valved/PLC/ID/PLCD16004. [Accessed 2026].

[19] CPC, “PLC42004 1/4 Hose Barb Non-Valved Panel Mount Coupling Insert,” CPC, 2026. [Online]. Available: https://www.cpcworldwide.com/General-Purpose/Products/Valved/PLC/ID/PLC42004#cad-download. [Accessed 2026].

[20] Bambu Lab, “PETG Basic Technical Data Sheet,” 2026.

[21] Bambu Lab, “PETG HF Technical Data Sheet,” 2026.

[22] Bambu Lab, “Bambu Filament Technical Data Sheet V3.0:PETG-CF,” [Online]. Available: https://store.bblcdn.com/626e4f424bf345ae965ad0ddfcaf2459.pdf.

[23] 3D Print Stuff, “Can FDM 3D Prints be Food Safe?,” 31 March 2023. [Online]. Available: https://www.youtube.com/watch?v=Nqj_F_XlRVY.

[24] Bambu Lab, “Bambu Filament Technical Data Sheet V3.0: ABS,” [Online]. Available: https://store.bblcdn.com/s7/default/23b4cf2b83d5470bb96d19970b5f3ae8/Bambu_ABS_Technical_Data_Sheet_V3.pdf.

[25] Bambu Lab, “Bambu Filament Technical Data Sheet V3.0:PC,” [Online]. Available: https://store.bblcdn.com/3bf3be91a7164c86a7e5ceffb18ee21b.pdf.

[26] M. Posch, “Why Chopped Carbon Fiber in FDM Prints Is A Contaminant,” 21 December 2025. [Online]. Available: https://hackaday.com/2025/12/21/why-chopped-carbon-fiber-in-fdm-prints-is-a-contaminant/.

[27] GeekDetour, “BrickLayers: Interlocking Layers Post-Processing Script,” [Online]. Available: https://github.com/GeekDetour/BrickLayers.

[28] R. Rajan and A. B. Pandit, “Correlations to predict droplet size in ultrasonic atomization,” June 2001. [Online]. Available: https://www.sciencedirect.com/science/article/pii/S0041624X01000543.

[29] The Engineering ToolBox, “Surface Tension - Water in contact with air,” 2004. [Online]. Available: https://www.engineeringtoolbox.com/water-surface-tension-d_597.html.

[30] The Engineering ToolBox, “Water Density, Specific Weight and Thermal Expansion Coefficients - Temperature and Pressure Dependence,” 2003. [Online]. Available: https://www.engineeringtoolbox.com/water-density-specific-weight-d_595.html.

[31] M. C. Watson, “Fogponic plant growth system,” 25 November 2016. [Online]. Available: https://patentimages.storage.googleapis.com/01/a4/cd/cd4873b05e11ad/CA2892131A1.pdf.

[32] APC International, Ltd., “What is a piezo transducer?,” [Online]. Available: https://www.americanpiezo.com/knowledge-center/piezo-theory/whats-a-transducer/.

[33] Holtek Semiconductor Inc., “1.7MHz/24V/20W Humidifers,” [Online]. Available: https://www.holtek.com/page/applications/detail/WAS-1995.

[34] Farnell, [Online]. Available: https://uk.farnell.com/seeed-studio/101020090/water-atomization-module-arduino/dp/4007693.

[35] “Understanding Power, Intensity, and Amplitude in Ultrasound,” 15 March 2025. [Online]. Available: https://quizlet.com/study-guides/understanding-power-intensity-and-amplitude-in-ultrasound-db76c458-f628-4ec7-9a86-395551460f5f.

[36] R. Zhao, “Are there any vibration - Damping properties of stainless steel brackets?,” 15 May 2025. [Online]. Available: https://www.nouvelglobal.com/blog/are-there-any-vibration-damping-properties-of-stainless-steel-brackets-28544.html.

[37] “Ultrasonic cleaning is fast, efficient and effortless,” [Online]. Available: https://ultrazvukovivani.com/wp-content/uploads/Brochure.pdf.

[38] “Component Selection for Product Design: A Comprehensive Guide,” 23 Aug 2024. [Online]. Available: https://www.cpduk.co.uk/news/component-selection-for-product-design-a-comprehensive-guide.

[39] “Time-of-Flight (ToF) ranging sensor based on ST's FlightSense technology,” [Online]. Available: https://www.st.com/en/imaging-and-photonics-solutions/vl53l1x.html.

[40] “Gravity: Non-contact Capacitive Flexible Liquid Level Sensor,” [Online]. Available: https://www.dfrobot.com/product-2463.html.

[41] “RS PRO Miniature Flat Pack Magnetic Proximity Switch, 23 x 5.9mm,” [Online]. Available: https://int.rsdelivers.com/product/rs-pro/rs-pro-magnetic-proximity-sensor-ip67/2892099.

[42] “sht85,” [Online]. Available: https://sensirion.com/products/catalog/SHT85.

[43] “Whadda WPM421 Water Pump Kit Create Your Own Plant Watering System,” [Online]. Available: https://www.rapidonline.com/whadda-wpm421-water-pump-kit-create-your-own-plant-watering-system-73-4687.

[44] “8315100136,” [Online]. Available: https://www.digikey.co.uk/en/products/detail/ebm-papst-inc/8315100136/14305768.

[45] l. ada, “Adafruit Motor Shield V2,” Adafruit, 9 September 2025. [Online]. Available: https://learn.adafruit.com/adafruit-motor-shield-v2-for-arduino/powering-motors. [Accessed 15 April 2026].

[46] Fondriest Environmental, Inc., “Dissolved Oxygen,” 2013. [Online]. Available: https://www.fondriest.com/environmental-measurements/parameters/water-quality/dissolved-oxygen/.

[47] F. Bantis, N. Tostsidid , G. Zervoudakis, A. Koukounaras and A. Koulopoulos, “Root0Zone Heating Boosts the Production of Mini Romaine Lettuce Grown in Nutrient Film Technique and Aeroponics Systems,” 30 January 2026. [Online]. Available: https://pmc.ncbi.nlm.nih.gov/articles/PMC12899869/.

[48] P. Karnoutsos, D. Katsantonis, A. Gkotzamani, A. Koukounaras, T. Kotsopoulos, X. Pantazi and V. Fragos, “Plant-Driven Precision Irrigation in Aeroponics: Real-Time Turgor Sensing for Sustainable Lettuce Cultivation,” 2025. [Online]. Available: https://www.mdpi.com/2077-0472/15/18/1948.

[49] F. Heltha, Y. Yunidar, R. Syahyadi, M. Melinda, R. Azhari and E. Elizar, “IoT-Enhanced mechanical system for fogponic cultivation: Air circulation and environmental control,” 2024. [Online]. Available: https://e-jurnal.pnl.ac.id/polimesin/article/view/6183.

[50] Farnell, “Seeed Studio 101020090 Water Atomization Module,” 2026. [Online]. Available: https://uk.farnell.com/seeed-studio/101020090/water-atomization-module-arduino/dp/4007693.

[51] N. Kacjan-Marsic and J. Osvald, “Nitrate content in lettuce grown on aeroponics with different quantities of nitrogen in the nutrient solution,” 2002. [Online]. Available: https://www.researchgate.net/publication/250006736_Nitrate_content_in_lettuce_Lactuca_sativa_L_grown_on_aeroponics_with_different_quantities_of_nitrogen_in_the_nutrient_solution.

[52] P. Glasso, “Grove-Water Atomization data,” December 2024. [Online]. Available: https://forum.seeedstudio.com/t/grove-water-atomization-data/284706/6.

[53] Piezo Direct, “Piezo Atomizer-Piezo Mist Generators and Fine Mist Generator,” 2026. [Online]. Available: https://piezodirect.com/piezo-atomizer/.

[54] L. Rees, “How to maintain recommended humidity levels inside your home,” 26 February 2026. [Online]. Available: https://homesmarter.co.uk/heating-cooling/recommended-humidity-level/.

[55] Allen, R. Pereira, L. S. Raes, D. Smith and Martin, “Crop evapotranspiration - Guidelines of computing crop water requirements - FAO Irrigation and drainage paper 56,” 1998. [Online]. Available: https://www.fao.org/3/x0490e/x0490e07.htm.

[56] V. Michalcova and K. Kotrasova, “The Numerical Diffusion Effect on the CFD Simulation Accuracy of Velocity and Temperature Field for the Application of Sustainable Architecture Methodology,” 3 December 2020. [Online]. Available: https://www.mdpi.com/2071-1050/12/23/10173.

[57] N. K. Marsic and J. Osvald, “Nitrate content in lettuce (Lactuca sativa L.) grown on aeroponics with different quantities of nitrogen in the nutrient solution,” *Acta Argonomica Hungarica,* vol. 50, pp. 389-397, 2002.

[58] P. Shen, L. Wang, W. A. Qureshi and J. Gao, “Influence of Rhizosphere Temperature and Humidity Regulation on Rooting, Mortality, and Transplant Survival of Aeroponically Rapid Growth Mulberry Cutting,” *Agronomy,* vol. 15, no. 3, p. 583, 2025.

[59] Johnson and D. John, “How Plants Use Nutrients,” 1 August 2021. [Online]. Available: https://extension.wvu.edu/lawn-gardening-pests/news/2021/08/01/how-plants-use-nutrients.

[60] E. E. Schulte and K. A. Kelling, “Plant Analysis: a Diagnostic Tool,” [Online]. Available: https://www.extension.purdue.edu/extmedia/nch/nch-46.html.

[61] Penn State Extension, “Hydroponics Systems and Principles Of Plant Nutrition: Essential Nutrients, Function, Deficiency, and Excess,” 2 February 2026. [Online]. Available: https://extension.psu.edu/hydroponics-systems-and-principles-of-plant-nutrition-essential-nutrients-function-deficiency-and-excess.

[62] Walters, J. Kellie and J. Christopher, “Hydroponic Greenhouse Basil Production: Comparing Systems and Cultivars,” 2025. [Online]. Available: https://journals.ashs.org/view/journals/horttech/25/5/article-p645.xml.

[63] A. San and A. Charles, “Fogponics vs Hydroponics for Lettuce Growth,” September 2024. [Online]. Available: https://www.scribd.com/document/765360425/FOGPONICS#:~:text=delivering%20nutrients%20directly%20to%20plant,yields.

[64] J. L. Havlin, J. D. Beaton, S. L. Tisdale and W. L. Nelson, “Soil Fertility and Fertilizers,” 2003. [Online]. Available: https://acsess.onlinelibrary.wiley.com/doi/abs/10.2136/sssaj2003.2000.

[65] Shirley Aquatics, “What is an airstone and how to use them in your tank,” [Online]. Available: https://shirleyaquatics.co.uk/knowledge/what-is-an-airstone-and-how-to-use-them-in-your-tank/.

[66] L. Jingying and W. Hang, “Dissolved oxygen transfer along falling water jets with developing surface disturbance,” 2021. [Online]. Available: https://www.researchgate.net/publication/350179170_Dissolved_oxygen_transfer_along_falling_water_jets_with_developing_surface_disturbance#:~:text=Plunging%20jet%20is%20also%20considered,water%20%5B4%2C%205%5D.

[67] “Component Selection for Product Design: A Comprehensive Guide,” *CPD News,* 2024.

[68] B. Rayner, “How to Choose the Best Components For Your Product Designs,” [Online]. Available: https://intelligence.supplyframe.com/how-choose-best-components/.

[69] S. Sadanand, “Component Selection in Electronic System Design”.

[70] A. Mittal, N. Mangadoddy and R. Banerjee, “GBU based discrete element modeling for convex polyhedral shape particles: Development and validation,” 2024. [Online]. Available: https://www.sciencedirect.com/science/article/abs/pii/S0032591024010519#:~:text=Importantly%2C%20the%20proposed%20DEM%20method,fidelity%20and%20reliability%20of%20simulations..